

AD-A087 760

TECHNICAL  
LIBRARY

AD

AD-E400 394

CONTRACTOR REPORT ARLCD-CR-79025

**SENSITIVITY OF MOLTEN AND SOLID TNT CHARGES  
TO IMPACT BY PRIMARY STEEL FRAGMENTS**

**GEORGE PETINO, JR.**  
HAZARDS RESEARCH CORPORATION  
DENVER, NEW JERSEY

**MICHAEL F. LEONDI, PROJECT ENGINEER**

**PAUL D. PRICE, PROJECT LEADER**  
ARRADCOM, DOVER, NEW JERSEY

**AUGUST 1980**



**US ARMY ARMAMENT RESEARCH AND DEVELOPMENT COMMAND  
LARGE CALIBER  
WEAPON SYSTEMS LABORATORY  
DOVER, NEW JERSEY**

**APPROVED FOR PUBLIC RELEASE; DISTRIBUTION UNLIMITED.**

The views, opinions, and/or findings contained in this report are those of the author(s) and should not be construed as an official Department of the Army position, policy or decision, unless so designated by other documentation.

Destroy this report when no longer needed. Do not return it to the originator.

The citation in this report of the names of commercial firms or commercially available products or services does not constitute official endorsement or approval of such commercial firms, products, or services by the United States Government.



UNCLASSIFIED

SECURITY CLASSIFICATION OF THIS PAGE(When Data Entered)

19. KEY WORDS (Continued)

Maximum fragment velocity without detonation

20. ABSTRACT (Continued)

Results of this program indicate that solid TNT charges that are impacted by 14 gram fragments are significantly more sensitive to fragment impact than molten TNT charges. Solid TNT and solid Amatex were found to be equally sensitive to fragment impact for the uncovered acceptor test condition. The order of decreasing sensitivity to fragment impact for the three molten explosives tested, on this and the previous two programs, is Amatex, Composition B, and TNT. It appears that a relationship exists among the kinetic energy of the fragment, its impact area, and the threshold detonation velocity.

UNCLASSIFIED

SECURITY CLASSIFICATION OF THIS PAGE(When Data Entered)

## TABLE OF CONTENTS

	Page No.
Introduction	1
Experimental Program	2
Materials	2
Equipment	2
Description of Experiments	3
Description of Experimental Methods	4
Experimental Results	7
Discussion of Results	9
Conclusions	11
Recommendations	12
References	13
Distribution List	53

## TABLES

1	Combinations of parameters tested	14
2	Results of tests with 14 gram fragments (solid acceptors)	15
3	Results of tests with 14 gram fragments (molten acceptors)	17
4	Results of tests with 28 gram fragments (solid acceptors)	18
5	Results of tests with 28 gram fragments (molten acceptors)	20
6	Results of tests with 42 gram fragments (solid acceptors)	22
7	Results of tests with 42 gram fragments (molten acceptors)	23
8	Comparison of velocity data	25
9	Summary of fragment impact test results	26
10	Summary of maximum fragment velocities	27
11	Comparison of Amatex and TNT test results (uncovered acceptor charge)	28
12	Comparison of Amatex, Composition B and TNT test results	29

## FIGURES

1	Experimental set-up	30
2	Schematic of experimental set-up	31
3	Forty-two gram steel fragment, four surrounds, and Lucite buffer plate	32
4	Schematic of fragment propulsion system	33

5	Composition B booster configuration	34
6	Solid TNT acceptor charge	35
7	Fragment aiming technique	36
8	Fragment velocity vs. Lucite thickness	37
9	Post-run condition of typical witness plate, pan, and fragment after a negative test result on an uncovered, solid acceptor	38
10	Post-run condition of typical witness plate, pan, acceptor plate, and fragment after a negative test result on a covered, solid acceptor	39
11	Post-run condition of typical witness plate, pan, and fragment after a negative test result on an uncovered, molten acceptor	40
12	Post-run condition of typical witness plate, pan, acceptor plate, and fragment after a negative test result on a covered, molten acceptor	41
13	Post-run condition of typical witness plate, pan, acceptor plate, and fragment after a low order detonation of a molten acceptor	42
14	Post-run condition of typical witness plate and pan after a high order detonation of a solid acceptor	43
15	Plot of test results for uncovered, solid TNT	44
16	Plot of test results for uncovered, molten TNT	45
17	Plot of test results for solid TNT with 0.318 cm thick acceptor plate	46
18	Plot of test results for molten TNT with 0.318 cm thick acceptor plate	47
19	Comparison of test results for molten and solid TNT as a function of fragment weight per unit area	48

20	Comparison of minimum velocity for detonation of molten and solid TNT and Amatex as a function of fragment weight per unit area	49
21	Comparison of test results for TNT, Composition B and Amatex	50
22	Critical diameter test setup	51

## INTRODUCTION

The fragment impact experiments performed in this program are a continuation of the work presented in two previous reports (refs 2 and 3). Both the experiments covered in those reports and the experiments covered in this report are modeled after the work presented in reference 1, which covered the sensitivity of both cased and uncased solid charges of pentolite and cyclotol to impact by steel fragments.

The objective of this program was to investigate the sensitivity of molten and solid TNT to impact by non-spinning, primary steel fragments weighing 14 to 42 g (0.5 to 1.5 oz) and traveling at velocities up to 2,134 m/s (7,000 fps). Primary fragments are defined as those fragments that result from break-up of an explosive casing in the event of a detonation. Usually, these fragments are characterized by having high velocity and are comparatively small in size. Variables studied included the presence or absence of a steel acceptor plate, fragment weight per unit impact area, and the molten vs. solid physical state of the TNT. Results were analyzed by comparing minimum velocities for detonation to maximum velocities without detonation. The data for TNT were then compared to those previously obtained for Composition B and Amatex in order to determine which explosive was the most sensitive.

An attempt was made to establish a relationship between fragment weight per unit frontal area and threshold detonation velocity. Information derived from this program will be used to develop a mathematical model which can be used to predict the boundary velocity of high velocity fragments, with variable weight per unit frontal areas, impacting explosive charges that have either no acceptor plates or acceptor plates of varying thicknesses. The mathematical model will then be applied in the design of new explosive facilities, modernization of existing facilities and in any operations where it is desired to limit the effects of accidental detonations. The net result of this effort will be increased safety at explosive facilities and cost reductions through efficient design.

## EXPERIMENTAL PROGRAM

### Materials

The following materials were supplied by ARRADCOM for use in this test program:

- (1) Composition B, cast, cylindrical booster, 7.6 cm (3.0 in) diameter x 7.6 cm (3.0 in) long, Lot RDD78A000E118
- (2) TNT, cast in 12.7 cm (5.0 in) x 12.7 cm (5.0 in) x 7.6 cm (3.0 in) high, 304 stainless steel pans with 0.159 cm (0.063 in) thick side walls, Lot RDD78A000E119

Hazards Research Corporation furnished the following materials:

- (1) High Speed, B & W Reversal Film Type 2962, 16 mm x 122 m (400 ft) rolls, mfr. by GAF Corporation
- (2) E-83 blasting caps
- (3) A-5 booster pellet, 75 grams, 5.1 cm (2.0 in) diameter x 2.5 cm (1.0 in) long
- (4) Wooden test stands
- (5) Lucite buffer plates
- (6) Steel fragments, type 1020 H. R.
- (7) Steel surrounds, type 1020 H. R.
- (8) Steel acceptor plates, type 1020 H. R., 0.318 cm (0.125 in) thick x 20.3 cm (8 in) square
- (9) Steel witness plates, type 1020 H. R., 0.953 cm (0.375 in) thk. x 20.3 cm (8.0 in) square

### Equipment

Hazards Research Corporation supplied the following high speed camera system:

- (1) Model 16-51 NOVA high speed camera with 400 to 20,000 picture per sec prism
- (2) Model 16-301, 122 m (400 ft) film magazine
- (3) Model 16-321 A balanced film spools, 122 m (400 ft) capacity

- (4) Model 1002 rectifier power supply, 120 volt AC, 60 cycle input with 140 to 150 volts DC to camera
- (5) Elgeet 15.2 cm (6 in), f: 3.8 lens
- (6) Model 2001 event timer
- (7) Model X-L exposure meter, 100 to 39,000 frames per sec, ASA 50 to 1600
- (8) Model 1005 timing light generator, 10, 100, 1000 pulses per sec output

### Description of Experiments

All experiments performed during this program were conducted using the experimental set-up shown pictorially in Figure 1 and schematically in Figure 2. The booster charge was composed of an E-83 cap, a 75 g A-5 pellet, and a 7.6 cm (3.0 in) diameter by 7.6 cm (3.0 in) long, Composition B charge. This entire explosive train was placed on top of a 12.7 cm (5.0 in) by 12.7 cm (5.0 in) square of Lucite of varying thickness. Glued to the opposite side of the Lucite was a square steel fragment of desired thickness and frontal area as shown in Figure 3. The fragment was surrounded by four pieces of equal thickness steel which prevent deformation at the edges of the fragment during the initial stages of launch. Figure 4 is a sketch which depicts the relative positions of the booster, Lucite, fragment and the surround. Figure 5 is a photo of the booster.

The entire fragment propulsion system was supported by a wooden stand that maintained a 145 cm (57 in) distance between the booster and the acceptor (target). There were two types of targets used on this program: solid and molten TNT. Each type had a 0.953 cm (0.375 in) thick by 20.3 cm (8.0 in) square witness plate on the underside of the charge. The experiments were conducted with or without a 0.318 cm (0.125 in) thick by 20.3 cm (8.0 in) square acceptor plate. Acceptor charges consisted of TNT cast in 12.7 cm (5.0 in) by 12.7 cm (5.0 in) by 7.6 cm (3.0 in) high, 304 stainless steel pans with 0.159 cm (0.063 in) thick side walls. Figure 6 is a photo of a solid TNT acceptor charge.

A typical test sequence started with the selection of: (a) the fragment velocity desired, (b) the Lucite thickness required to attain that velocity, (c) the physical state of the acceptor charge (molten or solid) and (d) the coverage mode of the acceptor (covered or uncovered). The booster charge was then placed on top of the stand, the fragment aimed at the center of the acceptor charge below, the cap armed and the event fired remotely by the high speed camera system. The camera was set up 27 meters (90 feet) away from the detonation site. Nominal camera speed was 20,000 pictures per second. The high speed camera was the only instrumentation used to record fragment velocity. Tests were valid only when film coverage was acceptable and the fragment impacted on the target area.

## Description of Experimental Methods

### Fragment Aiming Procedure

Figure 7 depicts the technique used to aim the fragment at the center of the receiver charge. The receiver is placed into position at the bottom of the test stand where it is leveled in two horizontal axes. A 20 cm square steel plate is then placed on top of the plywood platform. The plate has three equi-length plumb bobs suspended from three points 60 degrees apart. The plywood platform is adjusted in two horizontal axes until the tip of each plumb bob is exactly the same distance away from the acceptor cover plate. When this is accomplished, the plate is removed and the booster charge is placed into position on the plywood platform. The blasting cap is then connected to the firing circuit and the test set-up is ready to be fired by the camera.

### Fragment Calibration Firings

The results of the two previous programs were used as a basis for selecting the Lucite thicknesses required to achieve the specific fragment velocities desired on this program. Figure 9, from reference 2 and Figure 8, from reference 3, provided sufficient data to commence testing without performing any calibration firings. Figure 8 presents the results of the 90 tests performed during this experimental effort and provides a ready reference to the various fragment velocities attainable with a 7.6 cm diameter by 7.6 cm long Composition B booster.

### Fragment Velocity Measurement

The Nova high speed camera was used to record fragment velocity. It photographed the last 61 cm (24 in) of fragment travel, including fragment impact. The last 36 cm (14 in) of flight were marked off in 5 cm (2 in) increments on the vertical test stand support. Fragment velocity was computed in two ways. The first technique was to determine the elapsed time of fragment travel between the graduated 5 cm markings. Velocity was then computed by dividing the distance traversed by the time it took to traverse that distance. The second technique involved taking the starting time as that frame which was overexposed due to initiation of the booster. Impact at the steel acceptor plate marked the end of the event. Therefore, with the distance from the face of the fragment to the top of the acceptor plate known, the average velocity was calculated by dividing this distance by the elapsed time. Initial comparisons of the two techniques revealed that at the 1219 m/s (4000 fps) velocity level there was no significant difference in calculated velocities.

The advantage of the second technique is that lighting of the target area is not critical since initiation of the donor always overexposes the film and impact always results in a columnated beam of light emanating from the acceptor at impact. If impact results in a high order detonation, the detonation occurs within one frame. Since each frame is equal to 50 microseconds (at 20,000 frames per second), the detonation overexposes the film and obliterates the light given off by the columnation effect. Therefore, the high speed camera acts as a timer which is started and stopped by the light given off at initiation and impact.

As fragment velocities exceeded 1219 m/s (4000 fps), errors were introduced using the first technique due to blurring of the pictures of the fragment in flight. It was found that the second technique provided more accurate velocity data and it was decided that all velocity data reported would be that data generated using the second technique.

It should be noted that since the camera photographs in 50 microsecond increments, there is a slight error introduced in the time function. Initiation and impact each occur somewhere within a 50 microsecond time frame. Therefore, the time recorded could be up to 100 microseconds too long. At 1219 m/s (4000 fps), over the 145 cm flight path, an error of up to 112 m/s (368 fps) could result. It was decided that for the purposes of this program, this was not a large experimental error and it was deemed acceptable.

#### Preparation of Molten TNT Targets

Molten TNT acceptors were prepared by placing the cast TNT charges, steel acceptor plates (when required) and steel witness plates in a 110°C oven for 18 hours.

Prior to performing the first experiment, a series of tests were performed to determine the cooling rate of the acceptor with its hot steel plates in position. It was determined that no solidification occurred within a 5 minute period. All experiments were performed within this time frame.

The last operation performed during each test was the placing of the hot witness plate and molten TNT charge into position on the test stand. Extra molten TNT was added, as required, to allow it to overflow slightly. This eliminated the possibility of an air space developing between the top plate and the molten surface. After the hot, steel cover plate was placed into position, the cap was armed and fired.

## Characterization of Results of Fragment Impact

Impact of high velocity steel fragments on solid and molten TNT acceptors resulted in one of the following: no reaction, deflagration or detonation.

### No reaction

This result was characterized by shattered TNT strewn all over the floor of the test cell (solid acceptor), droplets of solidified explosive on the floor (molten acceptor), an intact steel pan, and a flat witness plate with a slight dent in it. In those tests that were performed with steel acceptor plates, the plates were bowed slightly at the point where the fragment passed through the plate. In most cases, the opening in the plate was square and generally conformed to the cross-section of the fragment. Figure 11 is a post-run photo of typical witness plate, pan, and fragment after a no reaction test result (test no. 20).

### Deflagration

Deflagrations were accompanied by clouds of smoke billowing out of the test cell and the recovery of all steel items in the condition described in the previous section. No physical evidence of the TNT remained after a deflagration. Figures 9, 10 and 12 show typical deflagration results for covered and uncovered solid acceptors and for a covered molten acceptor (test nos. 1, 45 and 57 respectively).

### Detonation

Detonations of both a low and high order class were considered to be positive results on this program. Low order detonations were characterized by the fracturing of the acceptor plate into two or more distorted pieces and the severe bowing of the witness plate. Bowing of 2 or more inches at the center of the witness plate was common. Some plates were bowed into crudely shaped hemispheres. Figure 13 is a photo which depicts the post-run condition of the steel plates after a low order detonation of a molten acceptor (test no. 19).

A high order detonation resulted in the complete shrapnellization of the cover plate. In addition, the witness plate was always driven downward into its wooden support. Its physical appearance was the mirror image of the explosive charge which rested on it. Specifically, a bowed, 12.7 cm square witness plate was always found with 3.8 cm (1.5 in) wide strips clearly sheared off around its outside edge. Figure 14 is a photograph which shows this typical post-run result (test no. 2).

## Experimental Results

A total of 87 primary steel fragment impact experiments were performed on this program. Table 1 presents the combinations of parameters tested and the number of experiments performed on each combination. It is seen that 44 tests were performed on solid TNT acceptors while 43 tests were performed on molten TNT acceptors. Tests were conducted with and without steel acceptor (cover) plates. When cover plates were used, the thickness was 0.318 cm. Tables 2 through 7 contain the detailed results of each test. A comparison of minimum velocity for detonation and maximum velocity without detonation for all combinations of parameters tested is presented in Table 8. Table 9 provides a summary of test program results. It allows a ready comparison of impact sensitivity for molten and solid TNT for both covered and uncovered acceptor charges. Figures 15 through 18 graphically present the data contained in Tables 2 through 7.

### Solid TNT Acceptor: 14 Gram Fragment

A series of 19 experiments were performed on solid acceptors using the 14 g (0.5 oz) fragment. Table 2 contains the results of these experiments. No cover plates were used for the first eight tests. The minimum velocity for detonation was found to be 1,647 m/s (5,404 fps) while the maximum velocity without detonation was 1,636 m/s (5,368 fps). Tests 9 through 19 used 0.318 cm thick acceptor plates which resulted in a 1,765 m/s (5,789 fps) minimum velocity for detonation and a 1,747 m/s (5,730 fps) maximum velocity without detonation. The steel plate increased the threshold velocity level by 118 m/s (387 fps).

### Molten TNT Acceptor: 14 Gram Fragment

Table 3 presents the results of 13 tests performed on this phase of the program. The first seven tests were performed on uncovered acceptors and resulted in a minimum velocity for detonation of 2,106 m/s (6,907 fps) and a maximum velocity without detonation of 1,919 m/s (6,293 fps). Tests 27 through 32 used the steel cover plates, resulting in a minimum velocity for detonation of 2,106 m/s (6,908 fps) and a maximum velocity without detonation of 2,052 m/s (6,730 fps). It is seen that there is no difference in threshold velocity level between covered and uncovered, molten TNT acceptor charges.

### Solid TNT Acceptor: 28 Gram Fragment

Fourteen experiments were performed on this phase of the program. Results of these tests are presented in Table 4. The minimum velocity for detonation of an uncovered, solid acceptor was found, after seven trials to be 1,361 m/s (4,465 fps). Maximum velocity without detonation was 1,308 m/s (4,291 fps). Seven additional tests were performed using the 0.318 cm thick, steel cover plates and resulted in a

minimum velocity for detonation of 1,398 m/s (4,584 fps) with a maximum velocity without detonation of 1,388 m/s (4,553 fps). The steel cover plate increased the threshold detonation velocity by 37 m/s (121 fps). This is an insignificant difference which indicates that the cover plate had no measureable effect on the threshold detonation velocity.

#### Molten TNT Acceptor: 28 Gram Fragment

A series of 15 tests were performed using 28 g (1.0 oz) fragments and molten acceptors. Table 5 contains the results of these experiments. No cover plates were used for the first seven experiments. The minimum velocity for detonation for these tests was found to be 1,808 m/s (5,930 fps) while the maximum velocity without detonation was 1,823 m/s (5,978 fps). Tests 54 through 61 used 0.318 cm thick acceptor plates which resulted in a 1,398 m/s (4,584 fps) minimum velocity for detonation and a 1,408 m/s (4,617 fps) maximum velocity without detonation.

#### Solid TNT Acceptor: 42 Gram Fragment

Table 6 presents the results of the eleven tests performed on this phase of the program. Seven tests on uncovered, solid acceptors resulted in a minimum velocity for detonation of 1,286 m/s (4,219 fps) and a maximum velocity without detonation of 1,282 m/s (4,205 fps). An additional four experiments performed using the 0.318 cm thick steel cover plates resulted in a minimum velocity for detonation of 1,270 m/s (4,167 fps) with a corresponding maximum velocity without detonation of 1,262 m/s (4,139 fps). For these experiments the difference between the threshold detonation velocities for uncovered and covered acceptors is insignificant.

#### Molten TNT Acceptor: 42 Gram Fragment

The last 15 experiments performed on this program are presented in Table 7. It is seen that nine tests were performed on uncovered, molten acceptors. These tests resulted in a minimum velocity for detonation of 1,332 m/s (4,370 fps) and a maximum velocity without detonation of 1,280 m/s (4,200 fps). Six tests were performed on 0.318 cm thick, steel cover plates. These resulted in a minimum velocity for detonation of 1,286 m/s (4,219 fps) and a maximum velocity without detonation of 1,303 m/s (4,274 fps). The effect of the steel cover plate is seen to be negligible since the difference in threshold velocities, 46 m/s (150 fps), is within the range of experimental error on this program.

## Discussion of Results

### Control of Fragment Velocity

The degree of control over fragment velocity attained on this program is evident if one analyzes the curves shown in Figure 8. It is seen that the majority of the data points were reproducible within about 152 m/s (500 fps). The broadest spread of data is on the order of 185 m/s (606 fps). Table 10 presents the maximum fragment velocities attained using the 7.6 cm diameter by 7.6 cm long, Composition B booster. As expected, fragment velocity decreases with increasing fragment weight.

### Effect of Fragment Weight Per Unit Impact Area

A fragment traveling at a constant velocity possesses a finite quantity of kinetic energy. At impact, this energy is transferred to the acceptor charge and is distributed across the impact surface area. The spacial orientation of the fragment at impact determines the impact area through which the kinetic energy is transmitted. The distribution of the kinetic energy across the face of the acceptor charge is one of the parameters that determines whether or not a detonation will occur. Visual observations of the high speed movies, acceptor pans, and steel plates from negative tests reveal that the majority of the fragments hit the acceptor charges in an essentially flat-on mode.

In order to allow a reasonable comparison of threshold velocity data among the three fragments tested, all data were analyzed by comparing fragment weight per unit area to threshold detonation velocity. Use of the term, fragment weight per unit area, implies that the frontal area of the fragment is equal to the impact area. One would expect that as the magnitude of the weight per unit area term increases, the threshold velocity level would decrease. This phenomenon does occur and can be seen in the results presented in Figures 15 through 19.

### Comparison of Test Results

Analysis of the data presented in Table 9 and Figure 19 reveals that the solid acceptors were more sensitive to fragment impact than the molten acceptors. This statement is valid for all three fragment weights in the uncovered acceptor charge tests and the 14 g fragment in the covered acceptor tests. There was no significant difference in sensitivity between molten and solid states for the covered acceptors when impacted by 28 and 42 g fragments.

Figure 19 also shows that the threshold detonation velocity decreased as the fragment weight per unit impact area increased for both molten and solid acceptors. The cover plate caused a significant difference in threshold velocity only in the case of the 28 g fragment.

Table 11 presents a comparison of Amatex and TNT test results for uncovered acceptor charges. The Amatex data was taken from the previous program (ref. 3). Figure 20 is a plot of the data found in Table 11. It is seen that there is no significant difference in sensitivity to fragment impact between TNT and Amatex for the solid charges. However, it is readily apparent that molten Amatex is much more sensitive than molten TNT. Threshold detonation velocity differences for the 14, 28 and 42 g fragments are 1141, 849 and 597 m/s (3,742, 2,785 and 1,958 fps) respectively.

Table 12 presents a comparison of Amatex, Composition B and TNT test results for acceptors covered by 0.318 cm thick steel plates. Figure 21 is a plot of the data presented in Table 12. Comparison of the molten acceptor data clearly reveals that Amatex is the most sensitive to primary fragment impact followed by Composition B and TNT. The data on solid acceptors reveals that, for the 14 g fragment, TNT and Composition B are more sensitive than Amatex. For the case of the 28 g fragment, the solid TNT is the most sensitive, with solid Amatex and solid Composition B having about the same threshold initiation levels. No data are available for Composition B at the 42 g fragment test point.

The test results in Figure 21 indicate that for the 14 g fragment and 0.318 cm acceptor plates, solid TNT is significantly more sensitive to primary fragment impact than molten TNT. This is the opposite of the results from similar Composition B and Amatex tests. A literature search has produced one test in which solid TNT appears more sensitive than molten TNT. Reference 5 reports that the critical diameter of solid flake TNT was less than 0.69 cm, while that of molten TNT was 1.6 cm. The critical diameter test is analagous to the tests conducted in this program since in both cases the target is subjected to high energy input levels. It is a severe shock case (Figure 22). The material with the lower critical diameter is considered to be the more sensitive of the two materials being evaluated.

These tests of TNT acceptors were conducted in the same manner and with the same test set-up as those of Composition B and Amatex acceptors. The fact that solid TNT was more sensitive than molten TNT in this high velocity impact test indicates further that the relative sensitivity of an energetic material is apparatus dependent. This is also demonstrated upon a review of the various sensitivity tests documented in Reference 5.

It must be remembered that the purpose of these tests is to investigate the sensitivity of molten and solid explosives to impact by primary steel fragments and any attempts to compare this data with other types of impact tests should not be binding since different methods rank the same explosives in different orders (Reference 6).

## CONCLUSIONS

As a result of the 87 primary steel fragment experiments performed on this program using both molten and solid TNT acceptors with and without steel cover plates, it is possible to conclude the following:

1. An empirical relationship has been established between fragment weight per unit impact area and threshold detonation velocity for the cases investigated on this program. The work conducted by previous investigators (References 1 and 4) has been extended to allow for the effects of impact area on threshold velocity.
2. Solid TNT is significantly more sensitive to impact by 14 gram fragments than molten TNT for both the covered and uncovered acceptor test conditions.
3. The 0.318 cm thick steel cover plate did not significantly increase the threshold detonation velocity level in either the molten or solid acceptor tests.
4. Threshold initiation velocities for both solid and molten TNT are inversely proportional to fragment weight per unit impact area.
5. Solid TNT and solid Amatex are equally sensitive to primary fragment impact for the uncovered acceptor test condition.
6. The order of decreasing sensitivity to fragment impact for the three molten explosives covered with a 0.318 cm thick steel cover plate is Amatex, Composition B and TNT.
7. The 7.6 cm diameter x 7.6 cm long Composition B launch system can propel 14, 28 and 42 gram steel fragments at maximum velocities of 2,180, 1,875 and 1,411 m/s (7,152, 6,150 and 4,628 fps) respectively.

## RECOMMENDATIONS

It is recommended that implementation of the following items be considered:

1. Use the data generated on this program to modify the mathematical equation for boundary velocity presented in References 1 and 4 by applying the effect of fragment weight per unit impact area on threshold detonation velocity.
2. Consider the application of this fragment explosive launch technique as a means of classifying the relative sensitivities of explosives, propellants and pyrotechnic materials to high velocity fragment impact. That is, consider this method as a standard hazards classification technique.
3. Perform primary fragment impact tests on uncovered, solid and molten Composition B acceptors and compare the results to those obtained for TNT and Amatex.
4. Duplicate this test effort using other solid and molten explosives and propellants at various stages of manufacture.
5. Perform primary fragment impact tests on highly confined TNT acceptor charges to determine the effect of confinement on threshold detonation velocity.

## REFERENCES

1. D. G. McLean and D. S. Allan, "An Experimental Program to Determine the Sensitivity of Explosive Materials to Impact by Regular Fragments," Report No. 64514, Arthur D. Little, Inc., Boston, MA, December 1965.
2. G. Petino, Jr., and D. DeMella, "Sensitivity of Cased Charges of Molten and Solid Composition B to Impact by Primary Steel Fragments," Technical Report 4975, Picatinny Arsenal, Dover, NJ, June 1976.
3. G. Petino, Jr., and M. Leondi, "Sensitivity of Molten and Solid Amatex Charges to Impact by Primary Steel Fragments," Contractor Report ARLCD-CR-78011, ARRADCOM, Dover, NJ, April 1978.
4. R. M. Rindner, "Establishment of Safety Design Criteria for Use in Engineering of Explosive Facilities and Operations, Report No. 2, Detonation by Fragment Impact," Technical Report DB-TR: 6-59, Picatinny Arsenal, Dover, NJ, May 1959.
5. T.W. Ewing et al., "A Compilation of Hazards Test Data for Propellants and Related Materials," Radford AAP, Hercules Inc., for US ARRADCOM, Dover, NJ, September 1976.
6. Engineering Design Handbook, Explosive Series, Explosive Trains, AMC Pamphlet AMCP 706-179, January 1974.

Table 1. Combinations of parameters tested for TNT

<u>Fragment weight</u>	<u>Fragment dimensions</u>	<u>Fragment wt/area</u>	<u>Acceptor plate thk.</u>	<u>Acceptor condition</u>	<u>No. of tests</u>
g (oz)	cm (in)	g/cm <sup>2</sup> (oz/in <sup>2</sup> )	cm (in)		
14 (0.5)	.32 x 2.36 x 2.35 (.125 x .930 x .930)	2.51 (0.58)	none none	solid molten	8 7
14 (0.5)	.32 x 2.36 x 2.35 (.125 x .930 x .930)	2.51 (0.58)	0.313 (0.125)	solid molten	11 6
28 (1.0)	.64 x 2.36 x 2.35 (.250 x .930 x .930)	5.02 (1.16)	none none	solid molten	7 7
28 (1.0)	.64 x 2.36 x 2.35 (.250 x .930 x .930)	5.02 (1.16)	0.313 (0.125)	solid molten	7 8
42 (1.5)	.94 x 2.40 x 2.40 (.370 x .945 x .945)	7.29 (1.67)	none none	solid molten	7 9
42 (1.5)	.94 x 2.40 x 2.40 (.370 x .945 x .945)	7.29 (1.67)	0.313 (0.125)	solid molten	4 6

Table 2. Results of tests with 14 gram fragments\*(solid TNT)

<u>Test no.</u>	<u>Lucite thk.</u> cm (in)	<u>Acceptor plate thk.</u> cm (in)	<u>Fragment velocity</u> m/s (fps)	<u>Remarks</u>
1	2.540 (1.000)	none	1,444 (4,736)	Deflagration
2	1.905 (0.750)	none	1,647 (5,404)	Detonation
3	1.905 (0.750)	none	1,636 (5,368)	Deflagration
4	1.588 (0.625)	none	2,000 (6,563)	Detonation
5	1.905 (0.750)	none	1,739 (5,703)	Detonation
6	2.540 (1.000)	none	1,539 (5,050)	Deflagration
7	2.540 (1.000)	none	1,479 (4,852)	Deflagration
8	1.956 (0.770)	none	1,679 (5,507)	Detonation
9	1.270 (0.500)	0.318 (0.125)	1,915 (6,280)	Detonation
10	0.953 (0.375)	0.318 (0.125)	2,038 (6,684)	Detonation
11	0.953 (0.375)	0.318 (0.125)	2,135 (7,004)	Detonation
12	1.270 (0.500)	0.318 (0.125)	1,883 (6,175)	Detonation

\*Fragment dimensions: 0.32 x 2.36 x 2.36 cm.

Table 2. Results of tests with 14 gram fragments\*  
(solid TNT) (cont.)

<u>Test no.</u>	<u>Lucite thk.</u> cm (in)	<u>Acceptor plate thk.</u> cm (in)	<u>Fragment velocity</u> m/s (fps)	<u>Remarks</u>
13	1.905 (0.750)	0.318 (0.125)	1,765 (5,789)	Detonation
14	2.540 (1.000)	0.318 (0.125)	1,568 (5,145)	Detonation
15	3.175 (1.250)	0.318 (0.125)	1,367 (4,485)	Deflagration
16	2.540 (1.000)	0.318 (0.125)	1,506 (4,941)	Deflagration
17	2.540 (1.000)	0.318 (0.125)	1,506 (4,941)	Deflagration
18	1.905 (0.750)	0.318 (0.125)	1,747 (5,730)	Deflagration
19	2.159 (0.850)	0.318 (0.125)	1,689 (5,541)	Deflagration

\*Fragment dimensions 0.32 x 2.36 x 2.36 cm.

Table 3. Results of tests with 14 gram fragments\* (molten TNT)

<u>Test no.</u>	<u>Lucite thk.</u> cm (in)	<u>Acceptor plate thk.</u> cm (in)	<u>Fragment velocity</u> m/s (fps)	<u>Remarks</u>
20	2.540 (1.000)	none	1,506 (4,940)	Deflagration
21	1.905 (0.750)	none	1,693 (5,553)	Deflagration
22	1.270 (0.500)	none	1,905 (6,250)	Deflagration
23	0.953 (0.375)	none	2,159 (7,080)	Detonation
24	0.953 (0.375)	none	2,111 (6,923)	Missed target
25	0.953 (0.375)	none	2,106 (6,907)	Detonation
26	1.270 (0.500)	none	1,919 (6,293)	Deflagration
27	1.905 (0.750)	0.318 (0.125)	1,771 (5,809)	Deflagration
28	1.270 (0.500)	0.318 (0.125)	1,883 (6,175)	Deflagration
29	1.270 (0.500)	0.318 (0.125)	2,052 (6,730)	Deflagration
30	0.953 (0.375)	0.318 (0.125)	2,180 (7,152)	Detonation
31	0.953 (0.375)	0.318 (0.125)	2,133 (6,995)	Detonation
32	0.919 (0.362)	0.318 (0.125)	2,106 (6,908)	Detonation

\*Fragment dimensions: 0.32 x 2.36 x 2.36 cm.

Table 4. Results of tests with 28 gram fragments\*( solid TNT)

<u>Test no.</u>	<u>Lucite thk.</u> cm (in)	<u>Acceptor plate thk.</u> cm (in)	<u>Fragment velocity</u> m/s (fps)	<u>Remarks</u>
33	1.270 (0.500)	none	1,251 (4,104)	Deflagration
34	0.635 (0.250)	none	1,545 (5,069)	Detonation
35	0.318 (0.125)	none	1,648 (5,404)	Detonation
36	0.953 (0.375)	none	1,489 (4,885)	Missed target
37	0.953 (0.375)	none	1,391 (4,562)	Detonation
38	1.270 (0.500)	none	1,308 (4,291)	Deflagration
39	0.953 (0.375)	none	1,361 (4,465)	Detonation
40	0.653 (0.250)	0.318 (0.125)	1,495 (4,908)	Detonation
41	0.318 (0.125)	0.318 (0.125)	1,705 (5,593)	Detonation
42	0.953 (0.375)	0.318 (0.125)	1,456 (4,776)	Deflagration
43	0.953 (0.375)	0.318 (0.125)	1,398 (4,584)	Detonation
44	1.270 (0.500)	0.318 (0.125)	1,388 (4,553)	Deflagration

\*Fragment dimensions: 0.64 x 2.36 x 2.36 cm.

Table 4. Results of tests with 28 gram fragments\*  
 (solid TNT) (cont.)

<u>Test no.</u>	<u>Lucite thk.</u> cm (in)	<u>Acceptor plate thk.</u> cm (in)	<u>Fragment velocity</u> m/s (fps)	<u>Remarks</u>
45	1.270 (0.500)	0.318 (0.125)	1,262 (4,139)	Deflagration
46	0.953 (0.375)	0.318 (0.125)	1,416 (4,647)	Detonation

\*Fragment dimensions: 0.64 x 2.36 x 2.36 cm.

Table 5. Results of tests with 28 gram fragments\* (molten TNT)

<u>Test no.</u>	<u>Lucite thk.</u> cm (in)	<u>Acceptor plate thk.</u> cm (in)	<u>Fragment velocity</u> m/s (fps)	<u>Remarks</u>
47	1.270 (0.500)	none	1,357 (4,450)	Deflagration
48	0.635 (0.250)	none	1,515 (4,968)	Deflagration
49	0.318 (0.125)	none	1,599 (5,245)	Deflagration
50	0.097 (0.038)	none	1,823 (5,978)	Deflagration
51	0.076 (0.030)	none	1,875 (6,150)	Detonation
52	0.318 (0.125)	none	1,713 (5,619)	Deflagration
53	0.076 (0.030)	none	1,808 (5,930)	Detonation
54	1.270 (0.500)	0.318 (0.125)	1,398 (4,584)	Detonation
55	1.905 (0.750)	0.318 (0.125)	1,165 (3,820)	Deflagration
56	1.905 (0.750)	0.318 (0.125)	1,156 (3,793)	Deflagration
57	1.270 (0.500)	0.318 (0.125)	1,286 (4,219)	Deflagration
58	0.953 (0.375)	0.318 (0.125)	1,408 (4,617)	Deflagration

\*Fragment dimensions: 0.64 x 2.36 x 2.36 cm.

Table 5. Results of tests with 28 gram fragments\*  
 (molten TNT) (cont.)

<u>Test no.</u>	<u>Lucite thk.</u> cm (in)	<u>Acceptor plate thk.</u> cm (in)	<u>Fragment velocity</u> m/s (fps)	<u>Remarks</u>
59	0.919 (0.362)	0.318 (0.125)	1,402 (4,600)	Missed target
60	0.635 (0.250)	0.318 (0.125)	1,595 (5,233)	Detonation
61	1.270 (0.500)	0.318 (0.125)	1,466 (4,808)	Detonation

\*Fragment dimensions: 0.64 x 2.36 x 2.36 cm.

Table 6. Results of tests with 42 gram fragments\*(solid TNT)

<u>Test no.</u>	<u>Lucite thk.</u> cm (in)	<u>Acceptor plate thk.</u> cm (in)	<u>Fragment velocity</u> m/s (fps)	<u>Remarks</u>
62	0.635 (0.250)	none	1,191 (3,907)	Deflagration
63	0.318 (0.125)	none	1,209 (3,967)	Deflagration
64	0.096 (0.038)	none	1,286 (4,219)	Detonation
65	0.152 (0.060)	none	1,366 (4,480)	Detonation
66	0.318 (0.125)	none	1,282 (4,205)	Deflagration
67	0.635 (0.250)	none	1,204 (3,950)	Deflagration
68	0.096 (0.038)	none	1,372 (4,500)	Detonation
69	0.318 (0.125)	0.318 (0.125)	1,228 (4,027)	Deflagration
70	0.152 (0.060)	0.318 (0.125)	1,270 (4,167)	Detonation
71	0.152 (0.060)	0.318 (0.125)	1,322 (4,336)	Detonation
72	0.318 (0.125)	0.318 (0.125)	1,262 (4,139)	Deflagration

\*Fragment dimensions: 3.94 x 2.40 x 2.40 cm.

Table 7. Results of tests with 42 gram fragments\* (molten TNT)

<u>Test no.</u>	<u>Lucite thk.</u> cm (in)	<u>Acceptor plate thk.</u> cm (in)	<u>Fragment velocity</u> m/s (fps)	<u>Remarks</u>
73	0.635 (0.250)	none	1,199 (3,933)	Deflagration
74	1.270 (0.500)	none	1,092 (3,582)	Deflagration
75	0.318 (0.125)	none	1,280 (4,200)	Deflagration
76	0.097 (0.038)	none	1,337 (4,384)	Detonation
77	0.076 (0.030)	none	1,411 (4,628)	Detonation
78	0.318 (0.125)	none	1,332 (4,370)	Detonation
79	0.635 (0.250)	none	1,237 (4,057)	Deflagration
80	0.940 (0.370)	none	1,068 (3,504)	Detonation
81	1.270 (0.500)	none	1,090 (3,575)	Deflagration
82	0.318 (0.125)	0.318 (0.125)	1,284 (4,210)	Deflagration
83	0.097 (0.038)	0.318 (0.125)	1,057 (3,466)	Deflagration
84	0.097 (0.038)	0.318 (0.125)	1,303 (4,274)	Deflagration

\*Fragment dimensions: 0.94 x 2.40 x 2.40 cm.

Table 7. Results of tests with 42 gram fragments\*  
(TNT acceptors) (cont.)

<u>Test no.</u>	<u>Lucite thk.</u> cm (in)	<u>Acceptor plate thk.</u> cm (in)	<u>Fragment velocity</u> m/s (fps)	<u>Remarks</u>
85	0.071 (0.028)	0.318 (0.125)	1,286 (4,219)	Detonation
86	0.076 (0.030)	0.318 (0.125)	1,375 (4,510)	Detonation
87	0.152 (0.060)	0.318 (0.125)	1,330 (4,361)	Detonation

---

\*Fragment dimensions: 0.94 x 2.40 x 2.40 cm.

Table 8. Comparison of velocity data for TNT

<u>Fragment weight</u> g (oz)	<u>Fragment wt/area</u> g/cm <sup>2</sup> (oz/in <sup>2</sup> )	<u>Acceptor plate thk.</u> cm (in)	<u>Acceptor condition</u>	<u>Min. vel. for det.</u> m/s (fps)	<u>Max. vel. without det.</u> m/s (fps)
14 (0.5)	2.51 (0.58)	none	solid	1,647 (5,404)	1,636 (5,368)
14 (0.5)	2.51 (0.58)	0.318 (0.125)	solid	1,765 (5,789)	1,747 (5,730)
14 (0.5)	2.51 (0.58)	none	molten	2,106 (6,907)	1,919 (6,293)
14 (0.5)	2.51 (0.58)	0.318 (0.125)	molten	2,106 (6,908)	2,052 (6,730)
28 (1.0)	5.02 (1.16)	none	solid	1,361 (4,465)	1,308 (4,291)
28 (1.0)	5.02 (1.16)	0.318 (0.125)	solid	1,398 (4,584)	1,388 (4,553)
28 (1.0)	5.02 (1.16)	none	molten	1,808 (5,930)	1,823 (5,978)
28 (1.0)	5.02 (1.16)	0.318 (0.125)	molten	1,398 (4,584)	1,408 (4,617)
42 (1.5)	7.29 (1.67)	none	solid	1,286 (4,219)	1,282 (4,205)
42 (1.5)	7.29 (1.67)	0.318 (0.125)	solid	1,270 (4,167)	1,262 (4,139)
42 (1.5)	7.29 (1.67)	none	molten	1,332 (4,370)	1,280 (4,200)
42 (1.5)	7.29 (1.67)	0.318 (0.125)	molten	1,286 (4,219)	1,303 (4,274)

Table 9. Summary of fragment impact test results for TNT

Fragment weight	Acceptor plate thk.	Min. vel. for det.		Max. vel. without det.	
		<u>solid</u>	<u>molten</u>	<u>solid</u>	<u>molten</u>
g (oz)	cm (in)	m/s (fps)	m/s (fps)	m/s (fps)	m/s (fps)
14 (0.5)	none	1,647 (5,404)	2,106 (6,907)	1,636 (5,368)	1,919 (6,293)
28 (1.0)	none	1,361 (4,465)	1,808 (5,930)	1,308 (4,291)	1,823 (5,978)
42 (1.5)	none	1,286 (4,219)	1,332 (4,370)	1,282 (4,205)	1,280 (4,200)
14 (0.5)	0.318 (0.125)	1,765 (5,789)	2,106 (6,908)	1,747 (5,730)	2,052 (6,730)
28 (1.0)	0.318 (0.125)	1,398 (4,584)	1,398 (4,584)	1,388 (4,553)	1,408 (4,617)
42 (1.5)	0.318 (0.125)	1,270 (4,167)	1,286 (4,219)	1,262 (4,139)	1,303 (4,274)

Table 10. Summary of maximum fragment velocities

<u>Fragment weight</u>	<u>Fragment dimensions</u>	<u>Max. fragment velocity</u>
g (oz)	cm (in)	m/s (fps)
14 (0.5)	.32 x 2.36 x 2.36 (.125 x .930 x .930)	2,180 (7,152)
28 (1.0)	.64 x 2.36 x 2.36 (.250 x .930 x .930)	1,875 (6,150)
42 (1.5)	.94 x 2.40 x 2.40 (.370 x .945 x .945)	1,411 (4,628)

Table 11. Comparison of Amatex and TNT test results  
(uncovered acceptor charge)

Fragment weight g (oz)	Acceptor condition*	Min. vel. for det.		Max. vel. without det.	
		TNT m/s (fps)	Amatex m/s (fps)	TNT m/s (fps)	Amatex m/s (fps)
14 (0.5)	solid	1,647 (5,404)	1,517 (4,978)	1,636 (5,368)	1,343 (4,405)
14 (0.5)	molten	2,106 (6,907)	965 (3,167)	1,919 (6,293)	814 (2,669)
28 (1.0)	solid	1,361 (4,465)	1,464 (4,803)	1,308 (4,291)	1,444 (4,739)
28 (1.0)	molten	1,808 (5,930)	959 (3,146)	1,823 (5,978)	857 (2,813)
42 (1.5)	solid	1,286 (4,219)	1,248 (4,094)	1,282 (4,205)	1,166 (3,825)
42 (1.5)	molten	1,332 (4,370)	735 (2,412)	1,280 (4,200)	673 (2,209)

\*Refer to Table 1 for number of trials for each acceptor condition.

Table 12. Comparison of Amatex, Composition B and TNT test results<sup>a</sup>

Frag. wt g (oz)	Acceptor <sup>b</sup> condition	Min. vel. for det.		Max. vel. without det.		
		Comp. B m/s (fps)	Amatex m/s (fps)	Comp. B m/s (fps)	Amatex m/s (fps)	TNT m/s (fps)
14 (0.5)	solid	1,767 (5,798)	1,956 (6,418)	1,587 (5,206)	1,913 (6,277)	1,747 (5,730)
14 (0.5)	molten	1,571 (5,155)	937 (3,075)	1,410 (4,626)	821 (2,692)	2,052 (6,730)
28 (1.0)	solid	1,651 (5,418)	1,711 (5,614)	1,377 (4,518)	1,648 (5,407)	1,388 (4,553)
28 (1.0)	molten	1,247 (4,090)	1,122 (3,682)	1,308 (4,292)	959 (3,146)	1,408 (4,617)
42 (1.5)	solid	-	1,248 (4,094)	-	1,166 (3,825)	1,282 (4,205)
42 (1.5)	molten	-	735 (2,412)	-	673 (2,209)	1,280 (4,200)
56 (2.0)	solid	1,323 (4,339)	-	1,352 (4,436)	-	-
56 (2.0)	molten	965 (3,166)	-	895 (2,937)	-	-

<sup>a</sup>Acceptor plate thickness: 0.318 cm (0.125 in).

<sup>b</sup>Refer to Table 1 for number of trials for each acceptor condition.

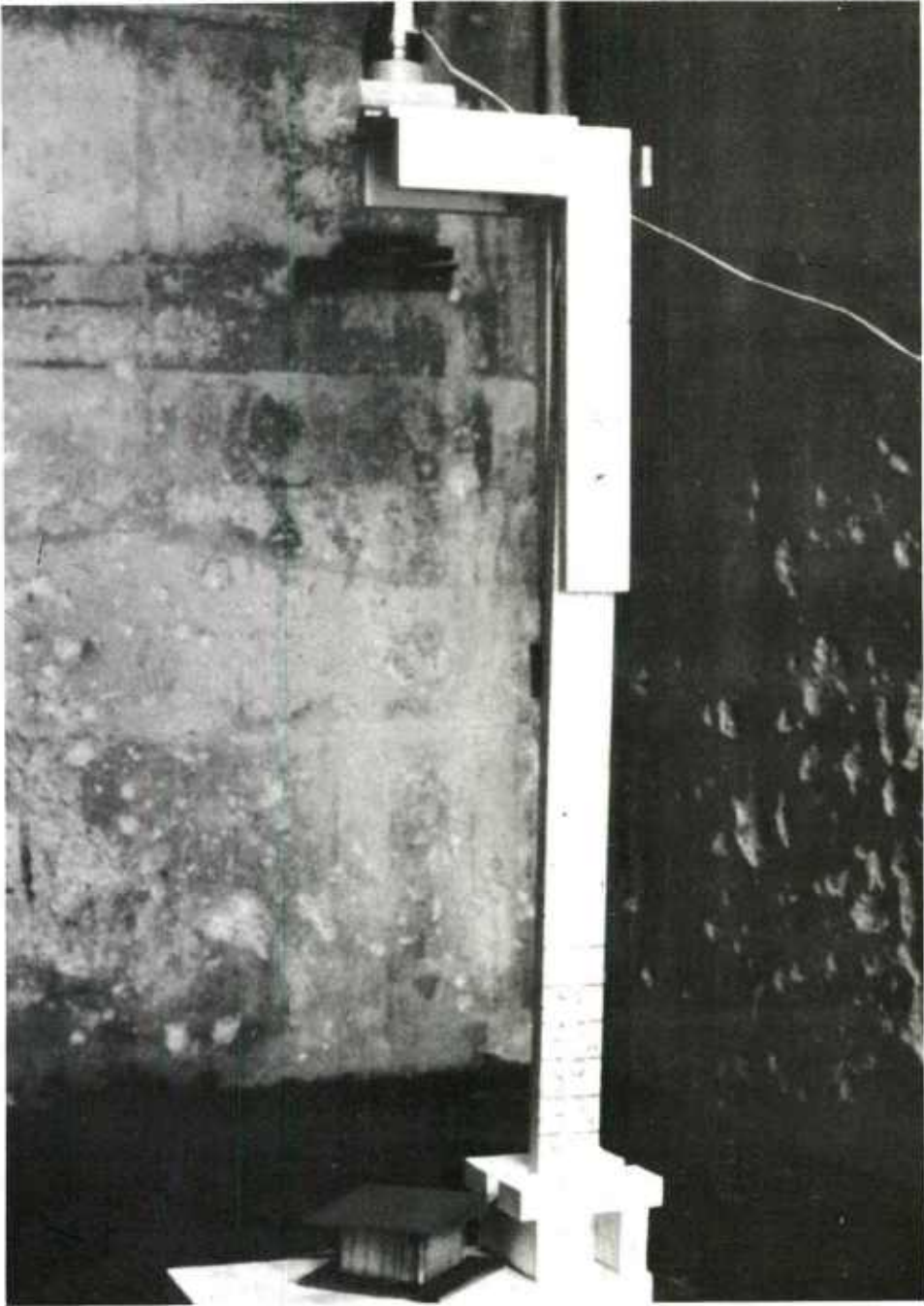


Figure 1. Experimental set-up.

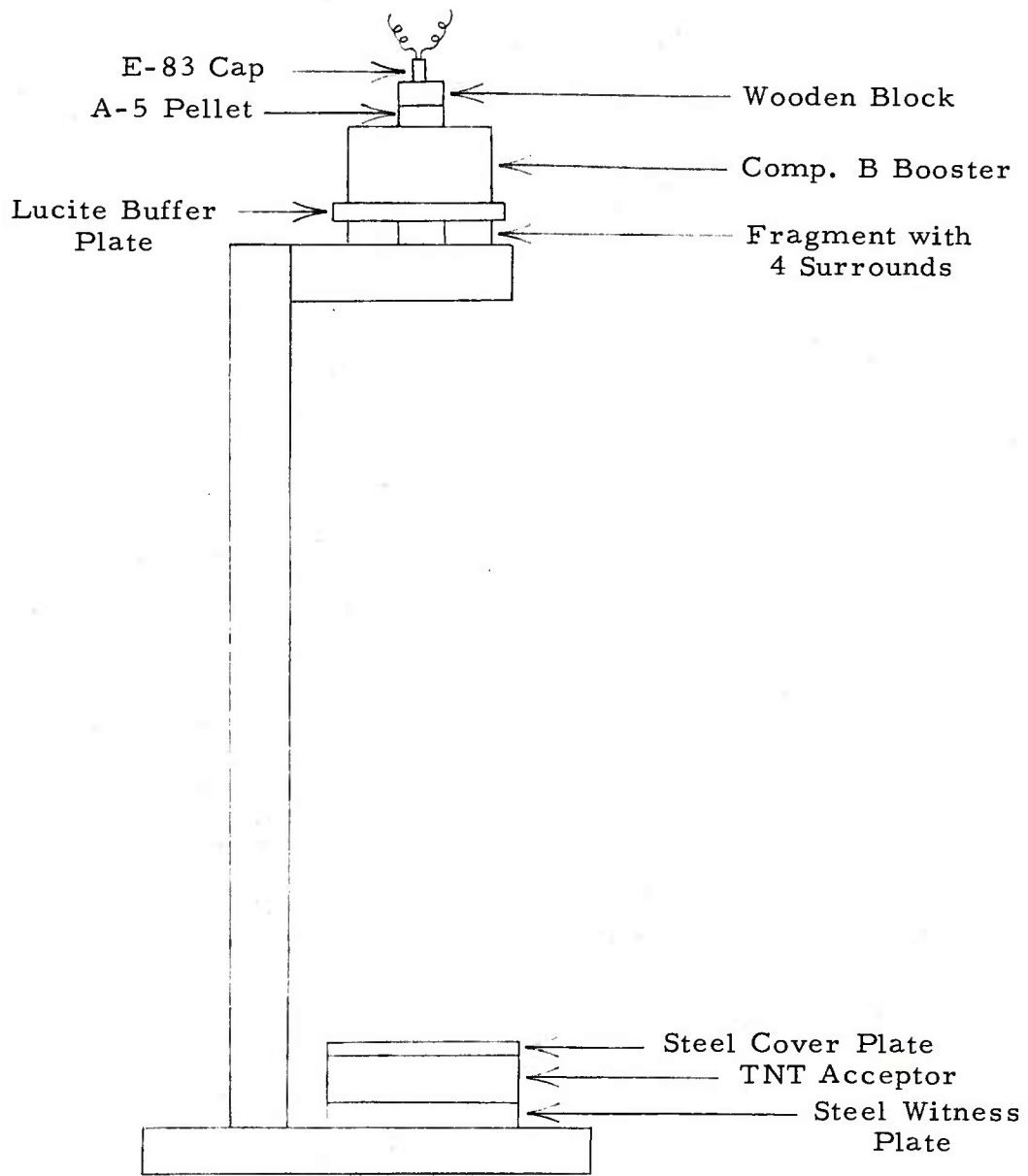


Figure 2. Schematic of experimental set-up.

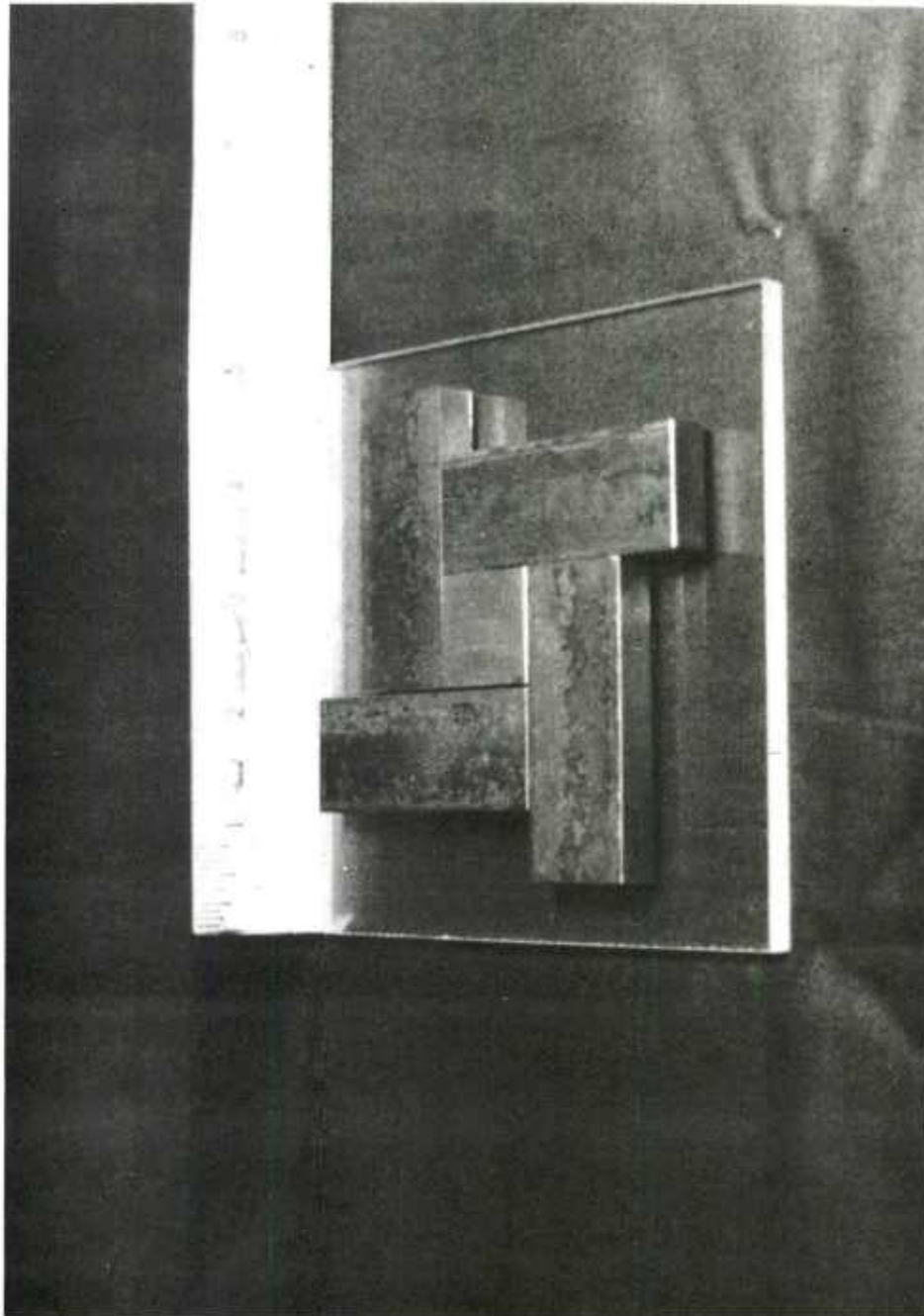


Figure 3. Forty-two gram steel fragment, four surrounds and Lucite buffer plate.

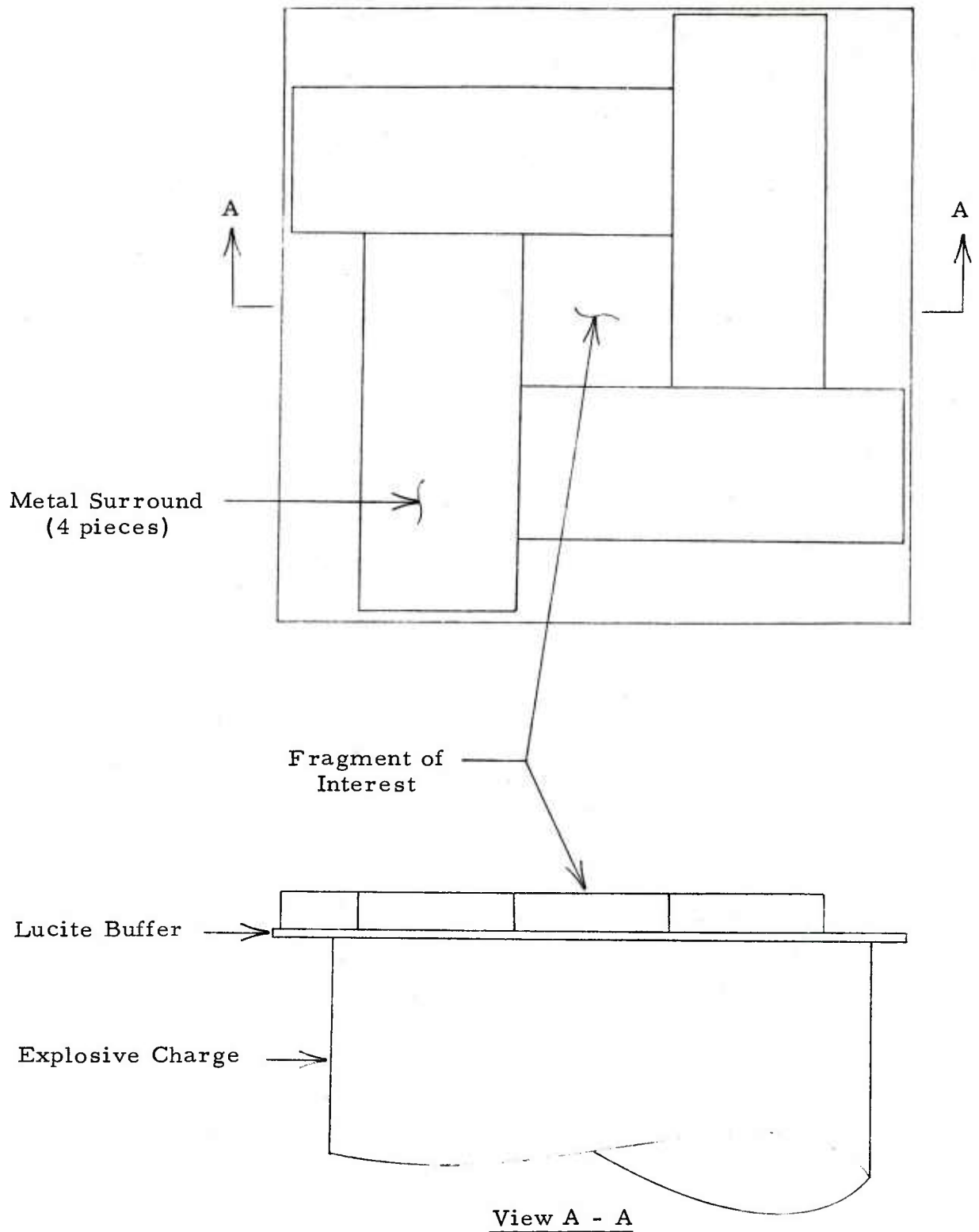


Figure 4. Schematic of fragment propulsion system.

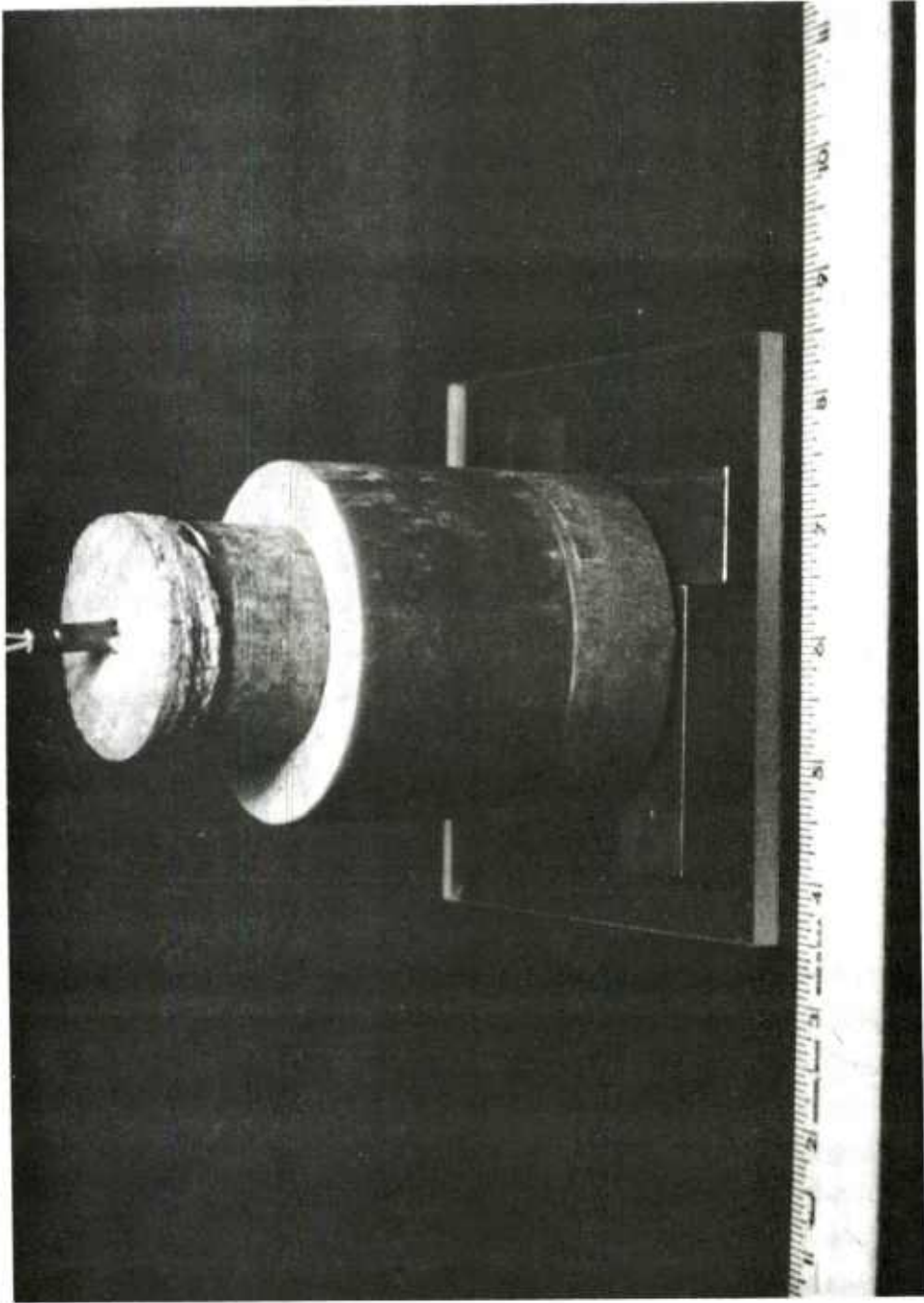


Figure 5. Composition B booster configuration.

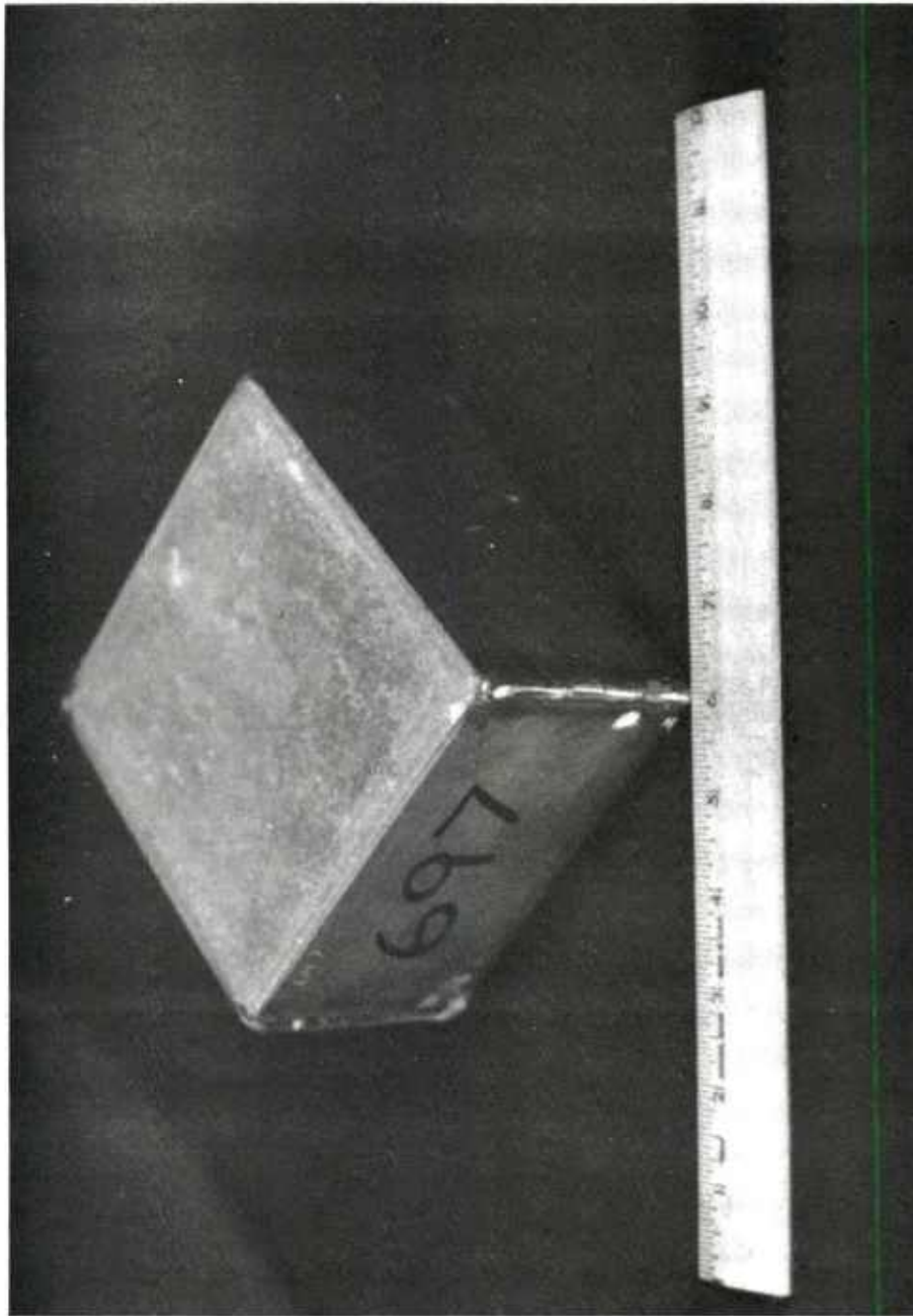


Figure 6. Solid TNT acceptor charge.

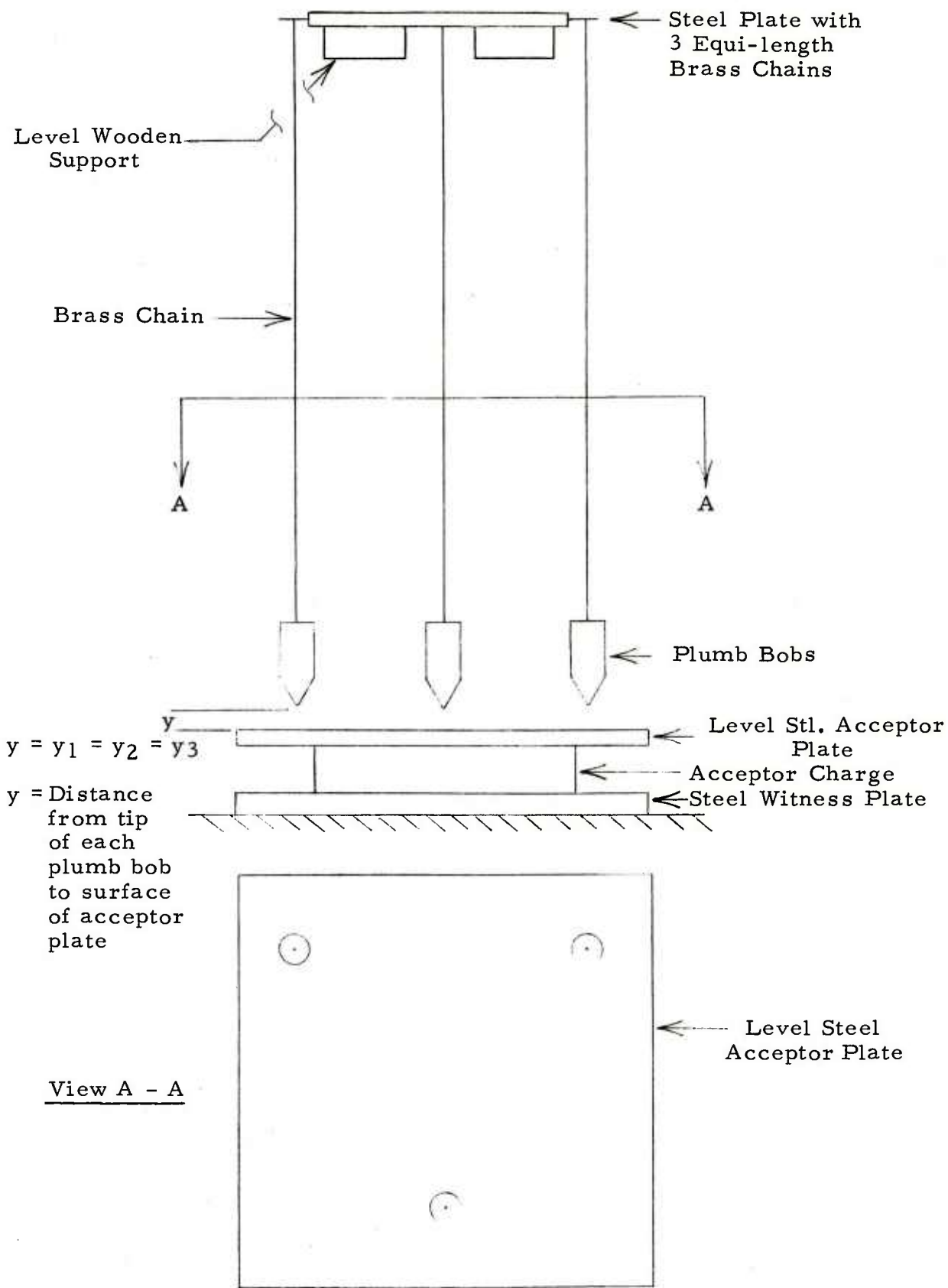


Figure 7. Fragment aiming technique.

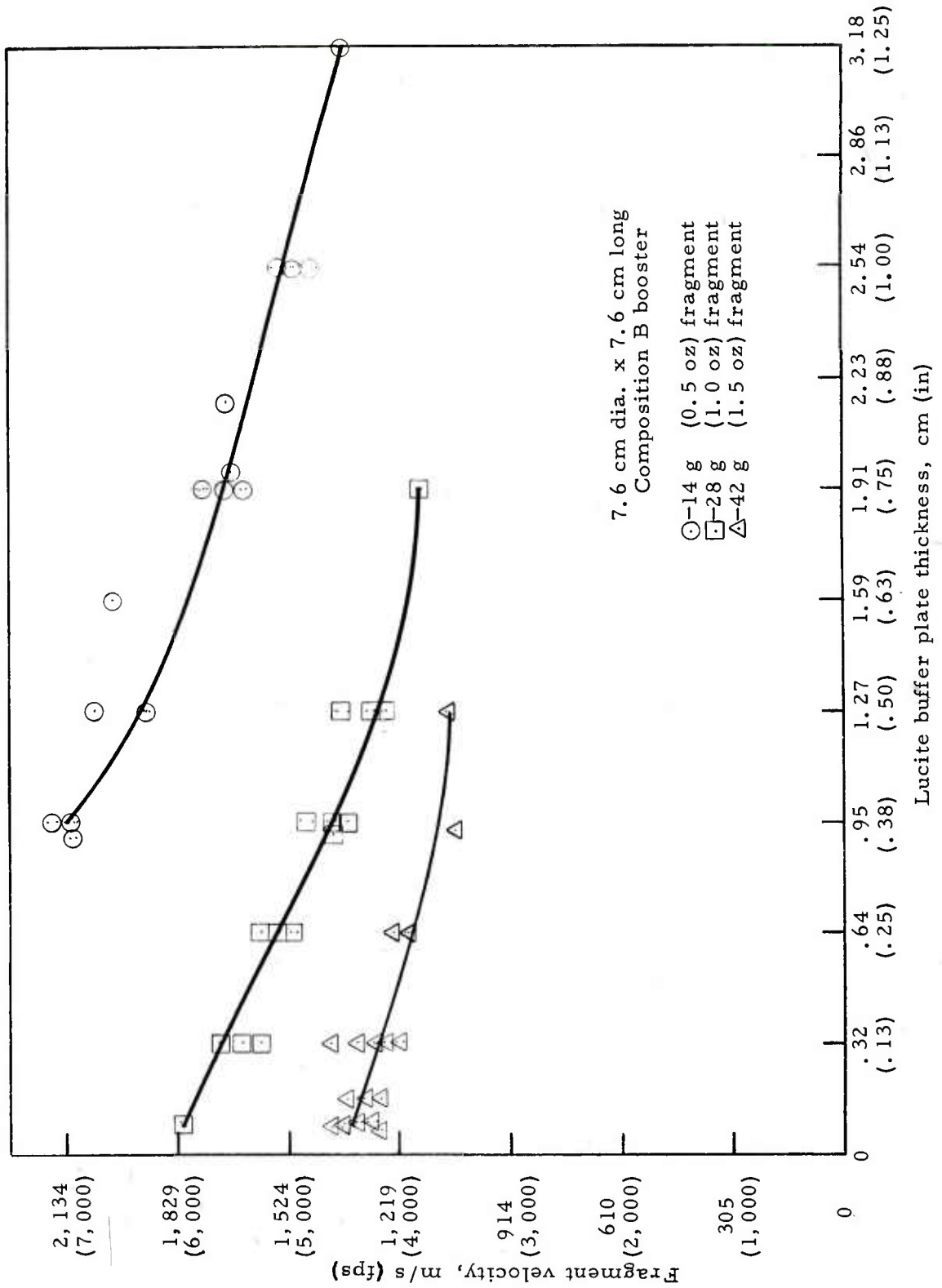


Figure 8. Fragment velocity vs Lucite thickness.

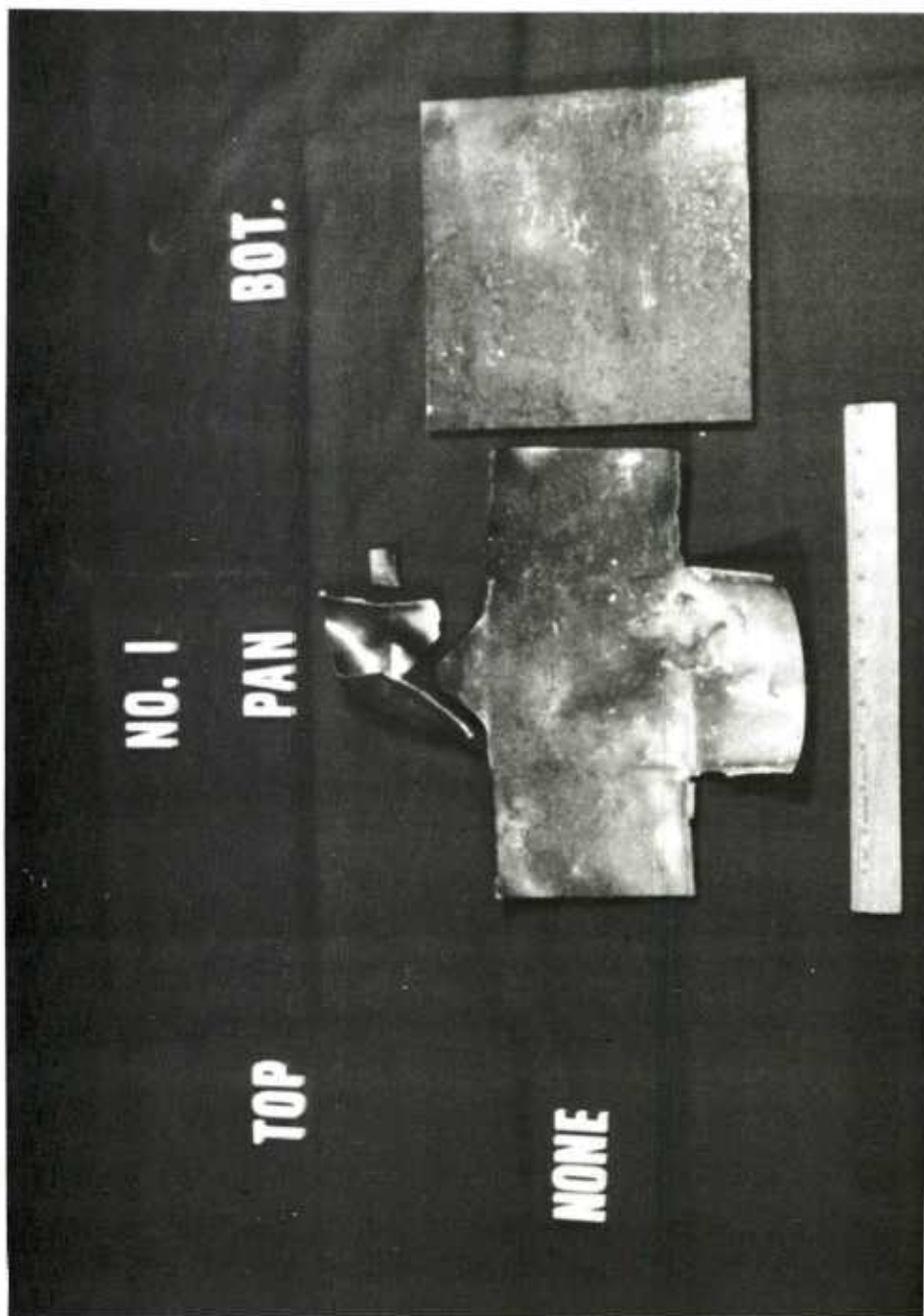


Figure 9. Post-run condition of typical witness plate, pan, and fragment after a negative test result on an uncovered, solid acceptor.

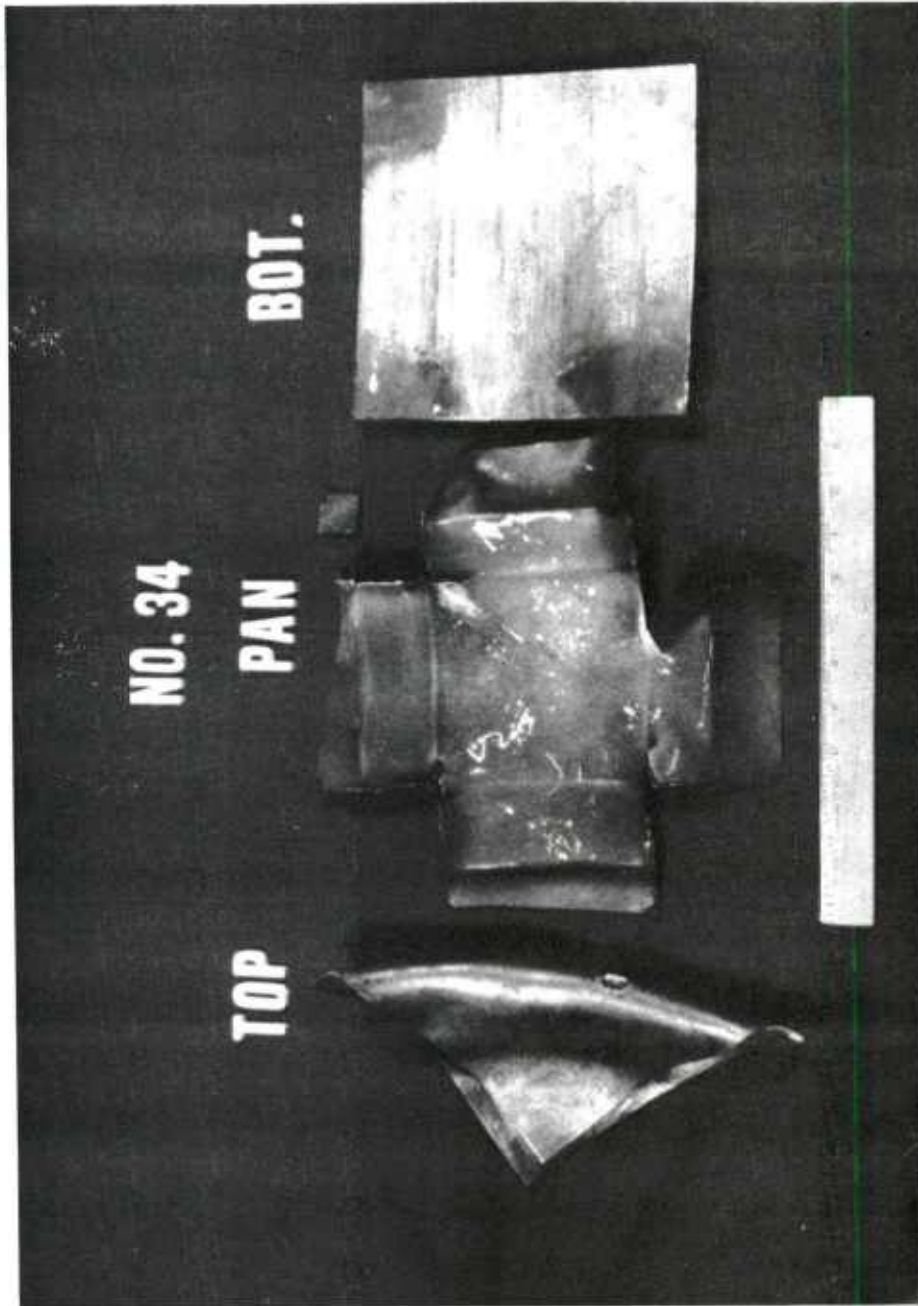


Figure 10. Post-run condition of typical witness plate, pan, acceptor plate, and fragment after a negative test result on a covered, solid acceptor.

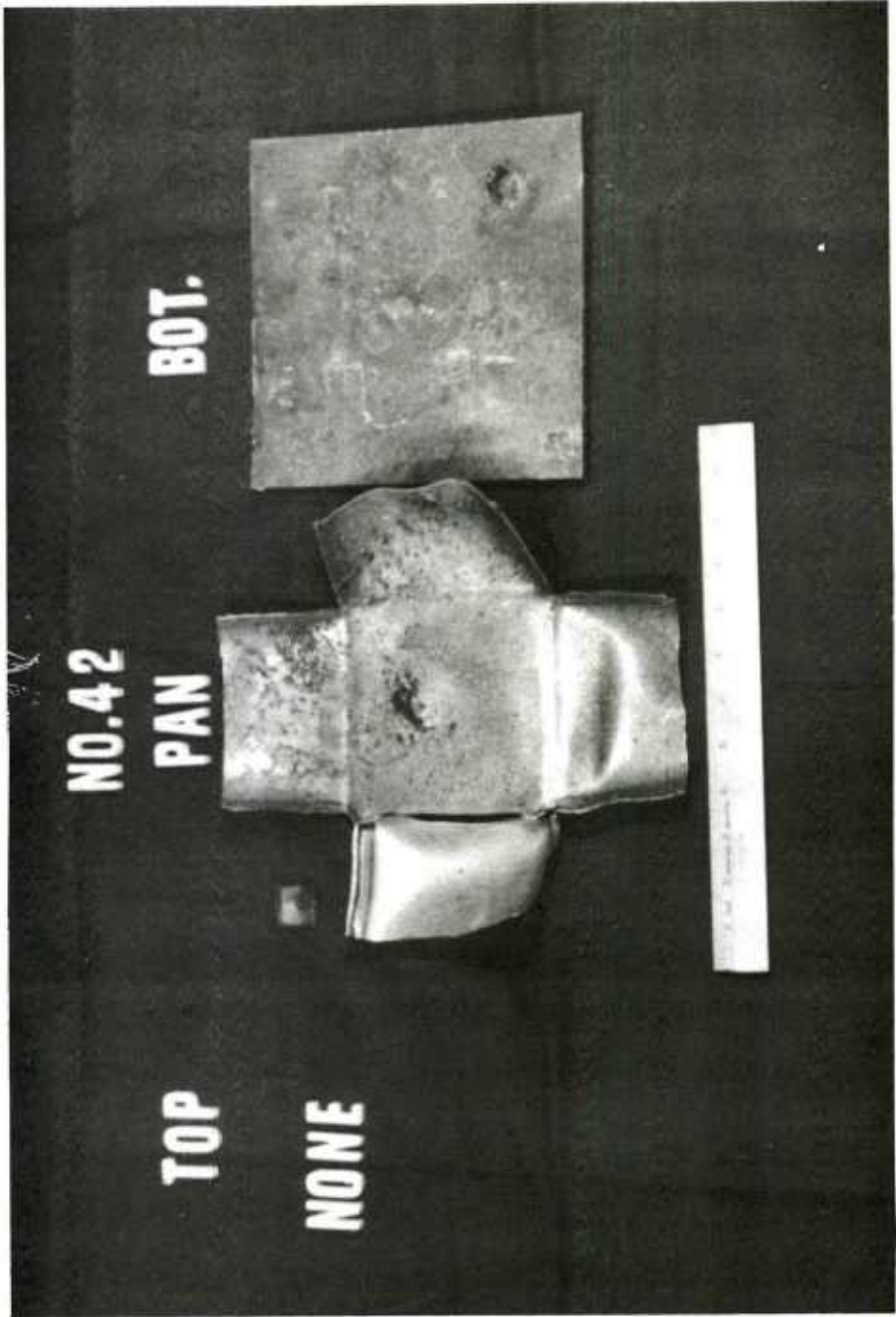


Figure 11. Post-run condition of typical witness plate, pan, and fragment after a negative test result on an uncovered, molten acceptor.

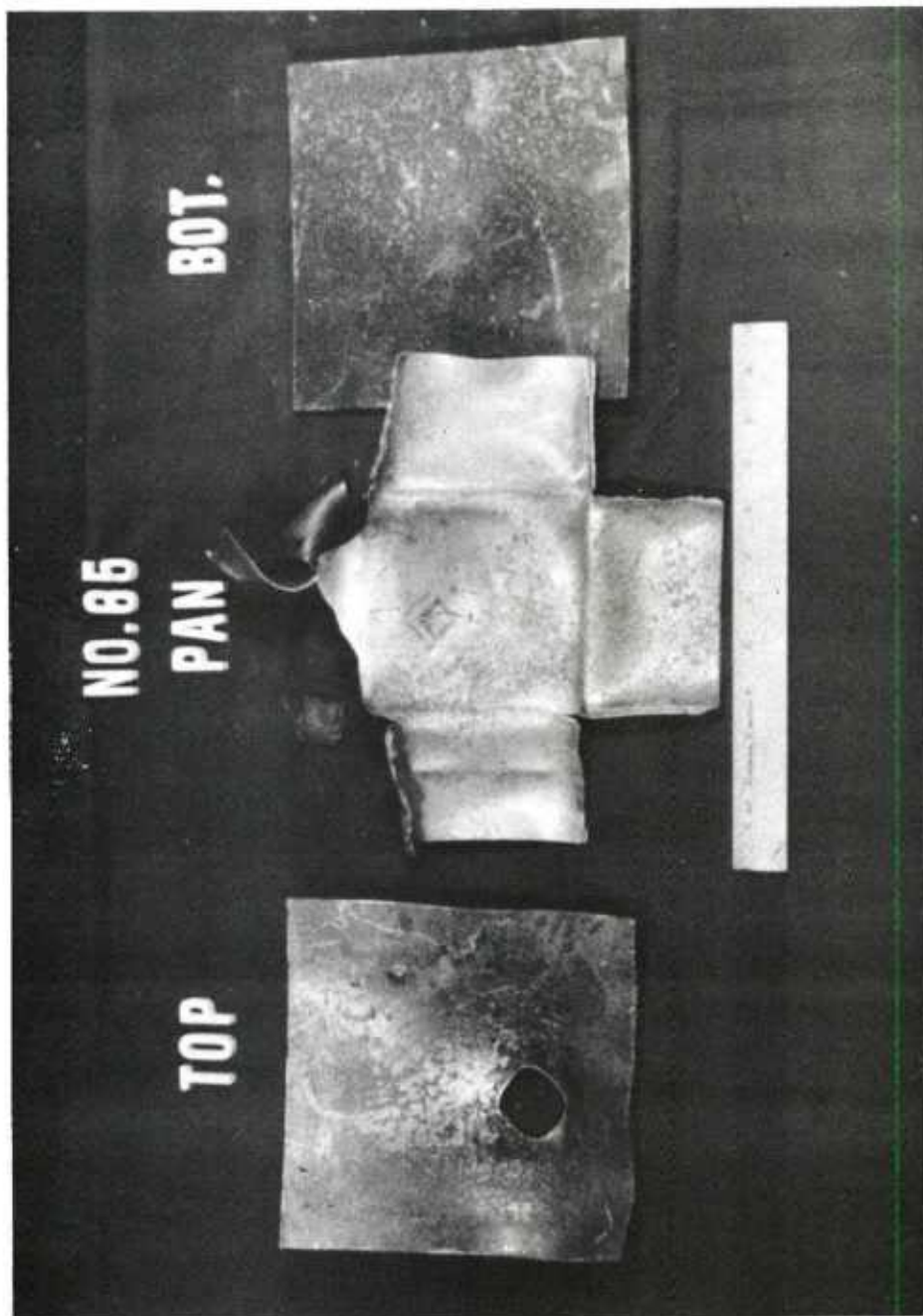


Figure 12. Post-run condition of typical witness plate, pan, acceptor plate and fragment after a negative test result on a covered, molten acceptor.

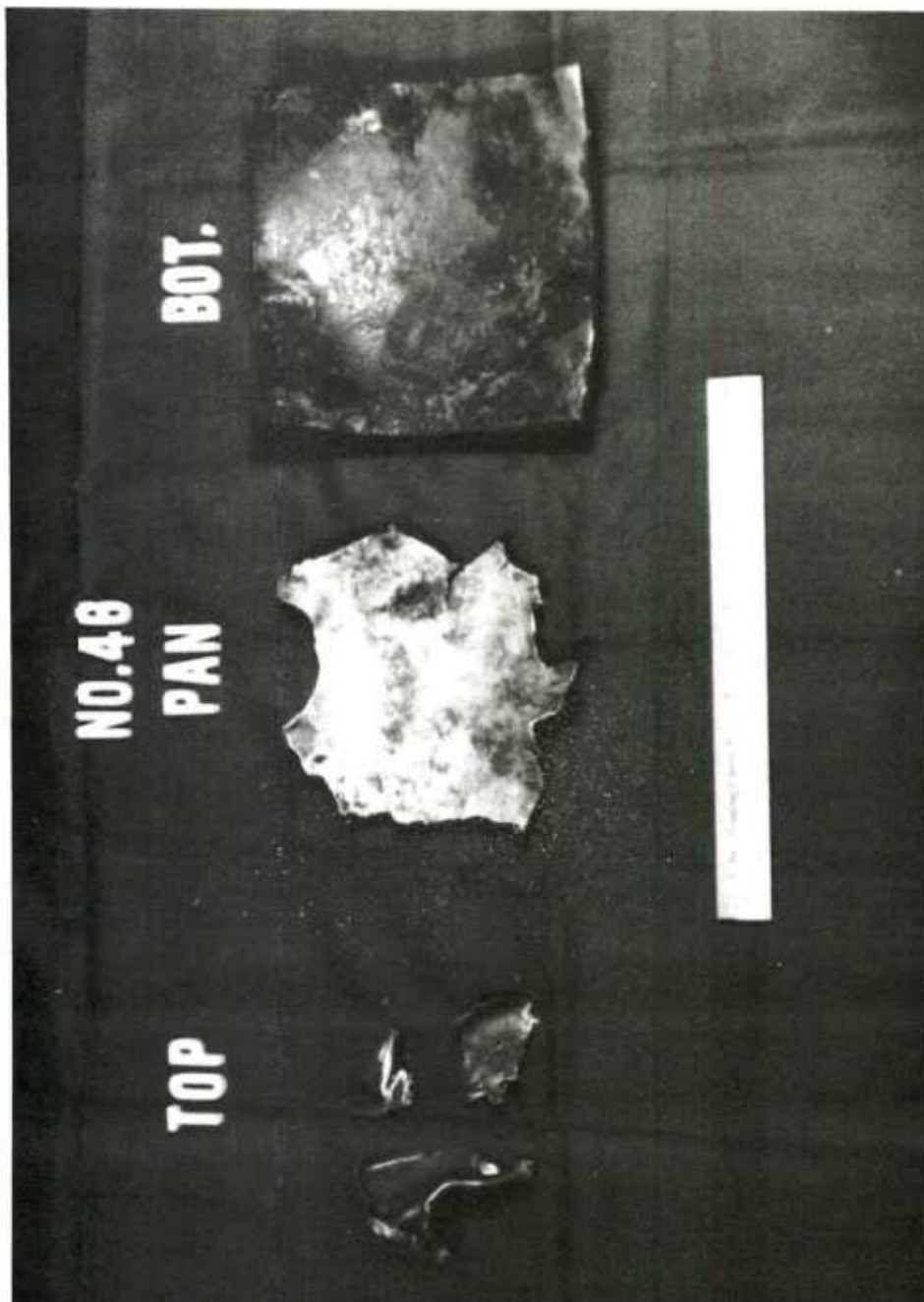


Figure 13. Post-run condition of typical witness plate, pan, acceptor plate, and fragment after a low order detonation of a molten acceptor.

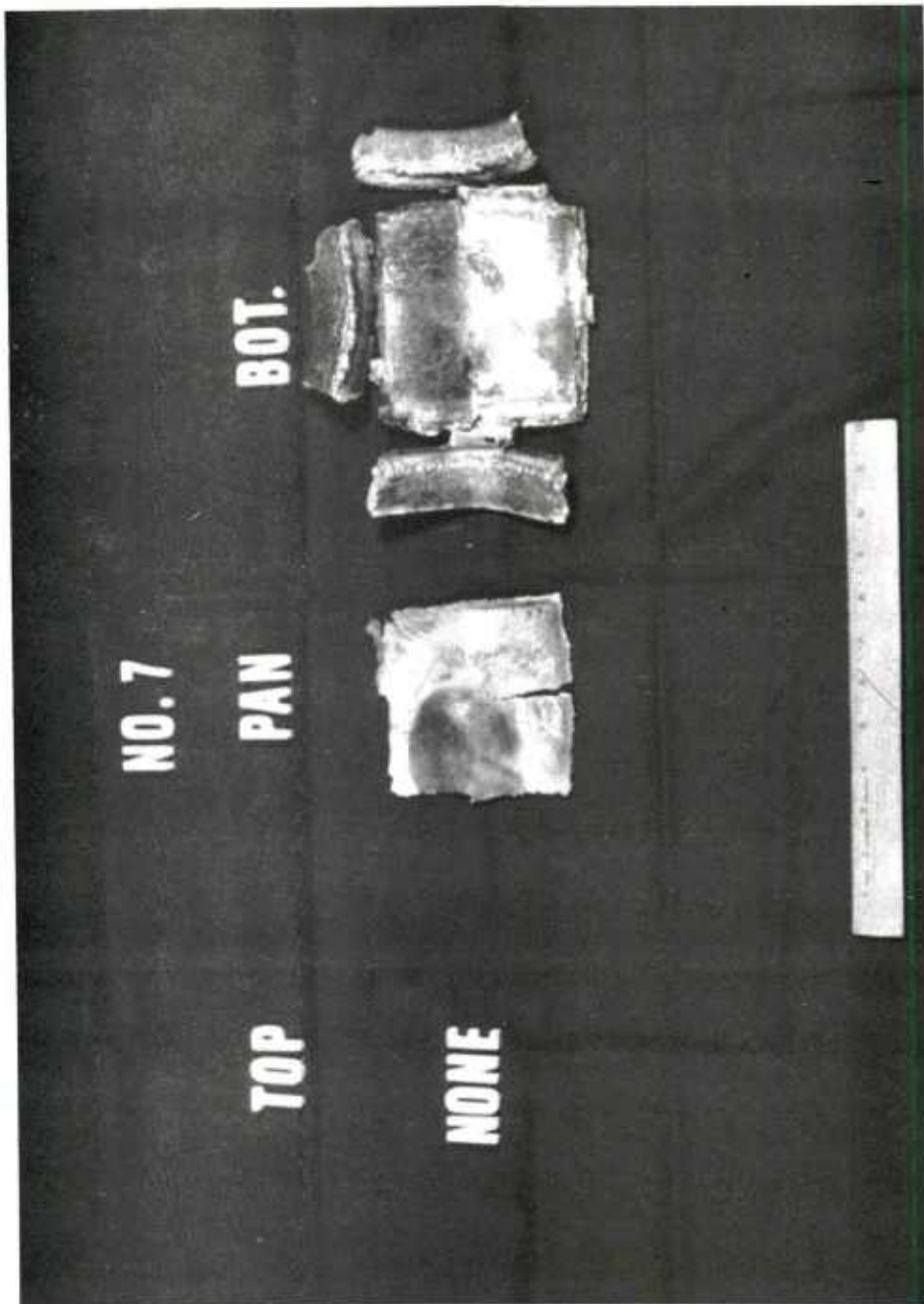


Figure 14. Post-run condition of typical witness plate and pan after a high order detonation of a solid acceptor.

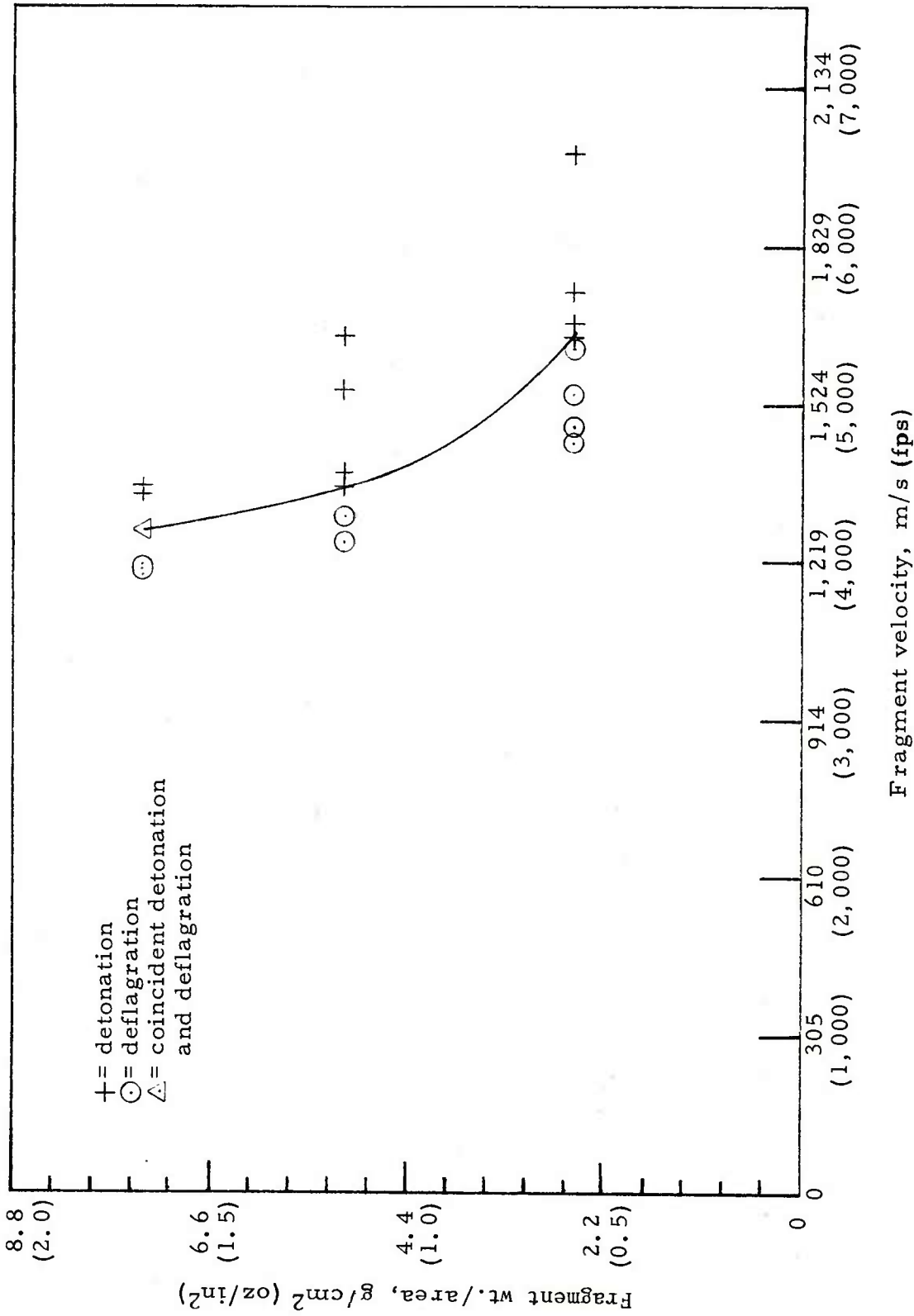


Figure 15. Plot of test results for uncovered, solid TNT.

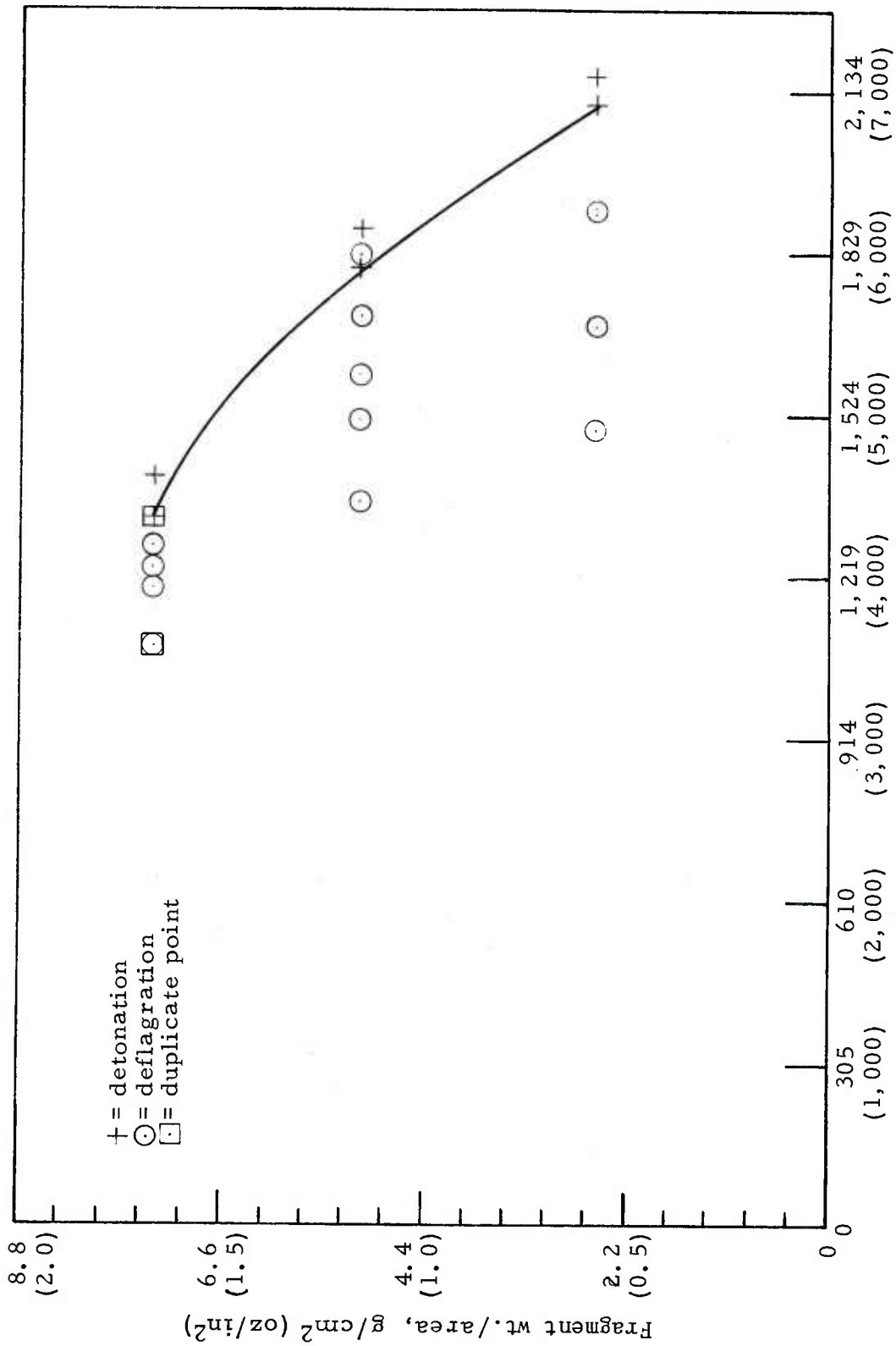


Figure 16. Plot of test results for uncovered, molten TNT.

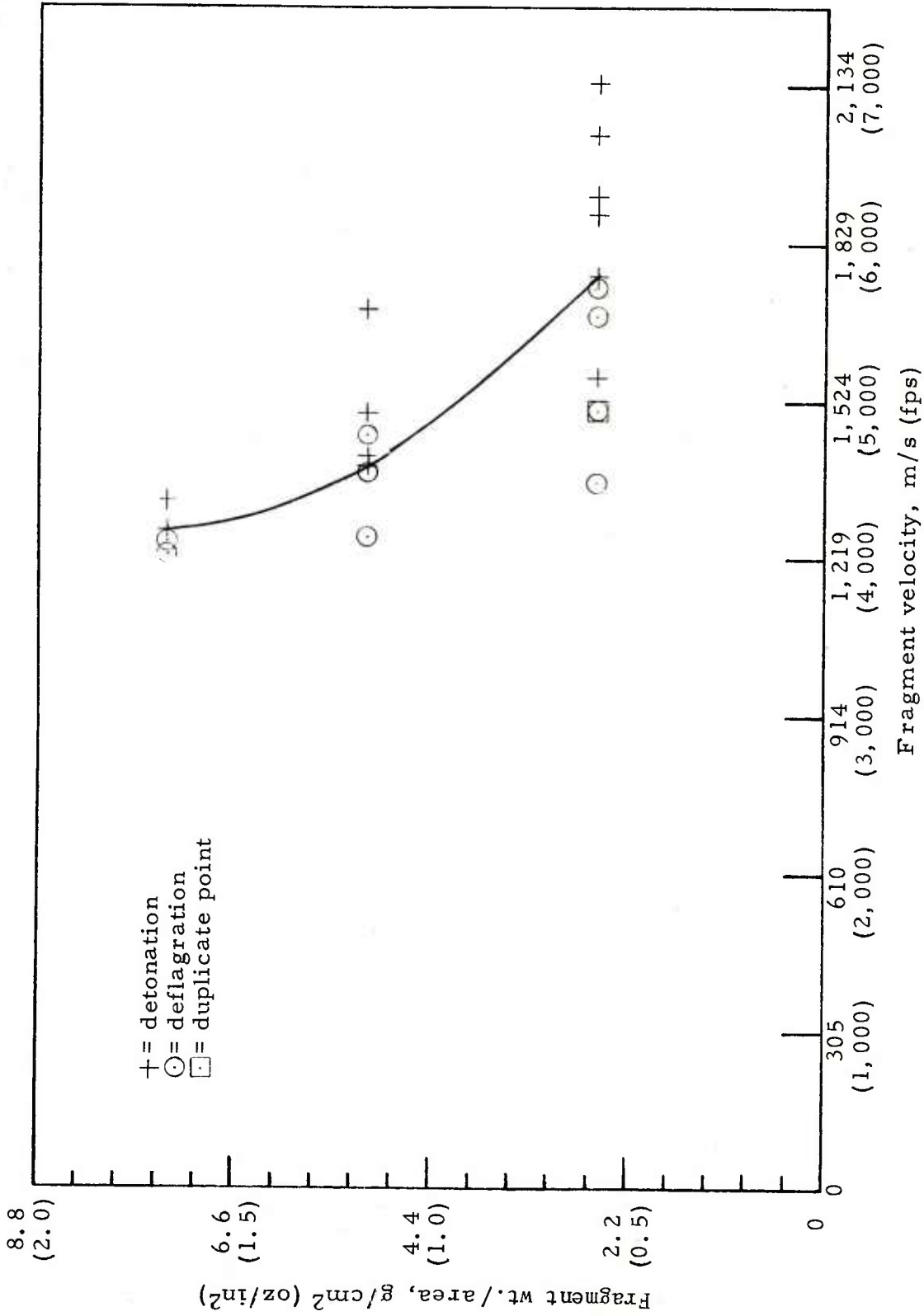
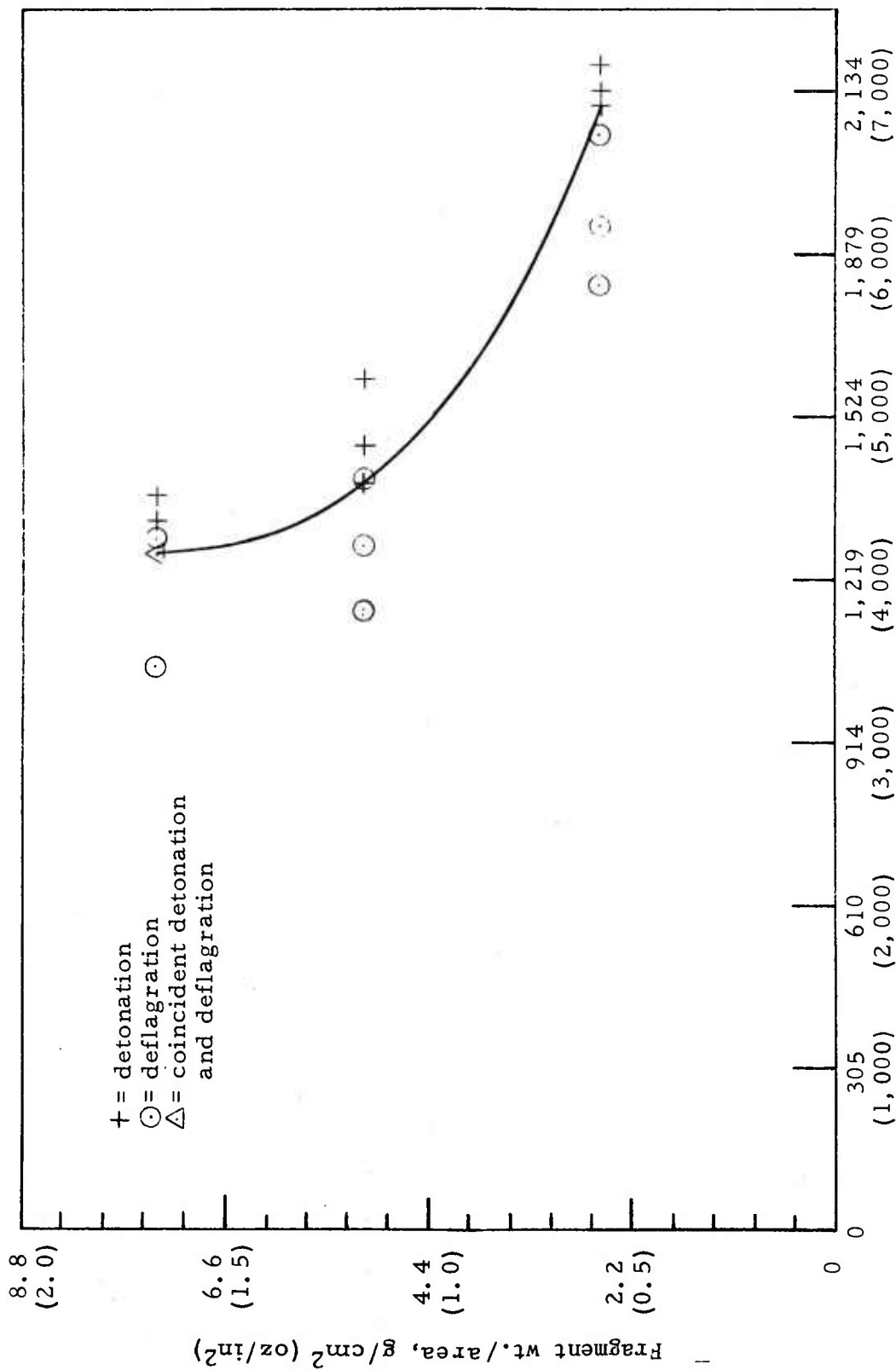
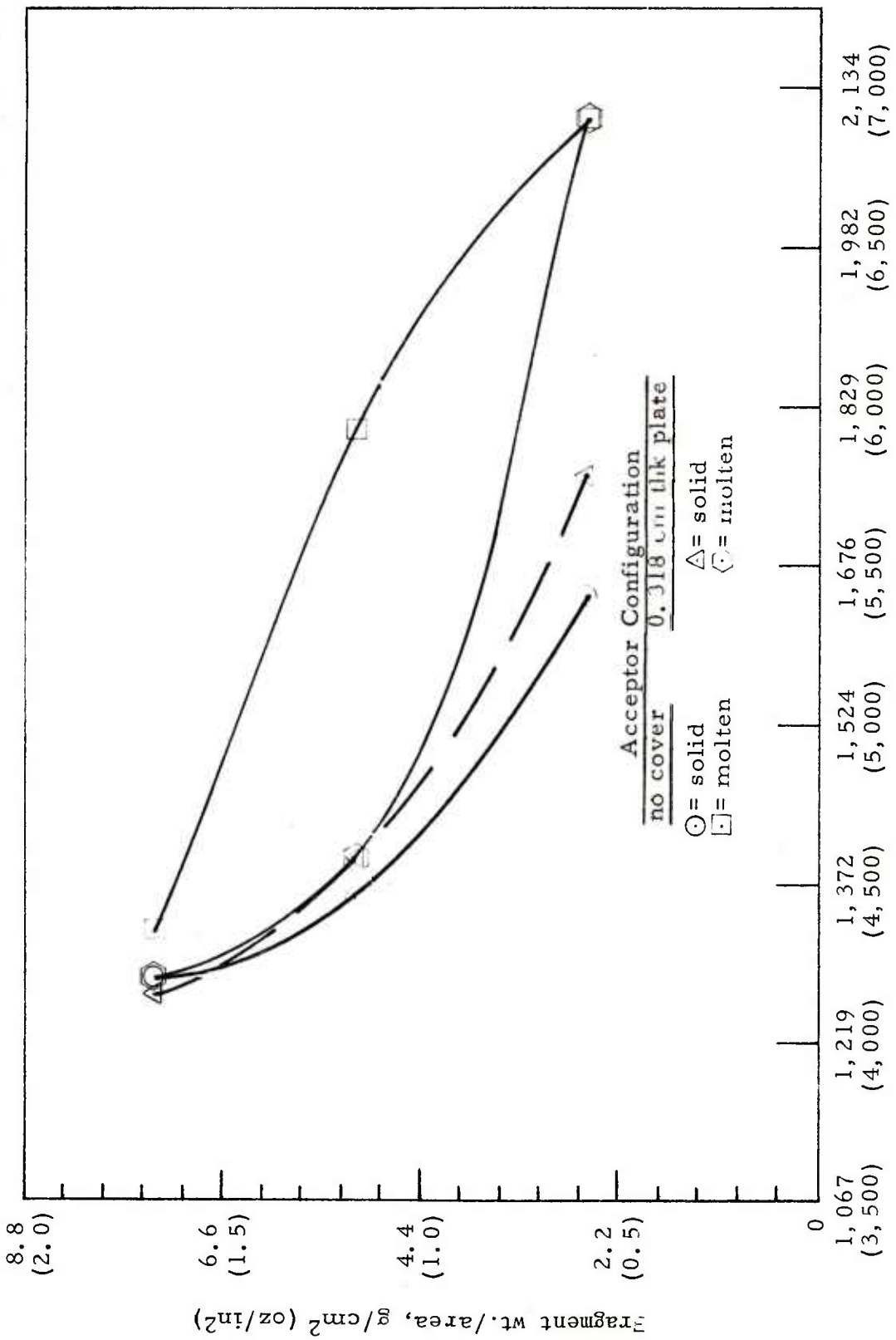


Figure 17. Plot of test results for solid TNT with 0.318 cm thick acceptor plate.



Fragment velocity, m/s (fps)

Figure 18. Plot of test results for molten TNT with 0.318 cm thick acceptor plate.



Fragment velocity, m/s (fps)

Figure 19. Comparison of minimum velocity for detonation of molten and solid TNT as a function of fragment weight per unit area.

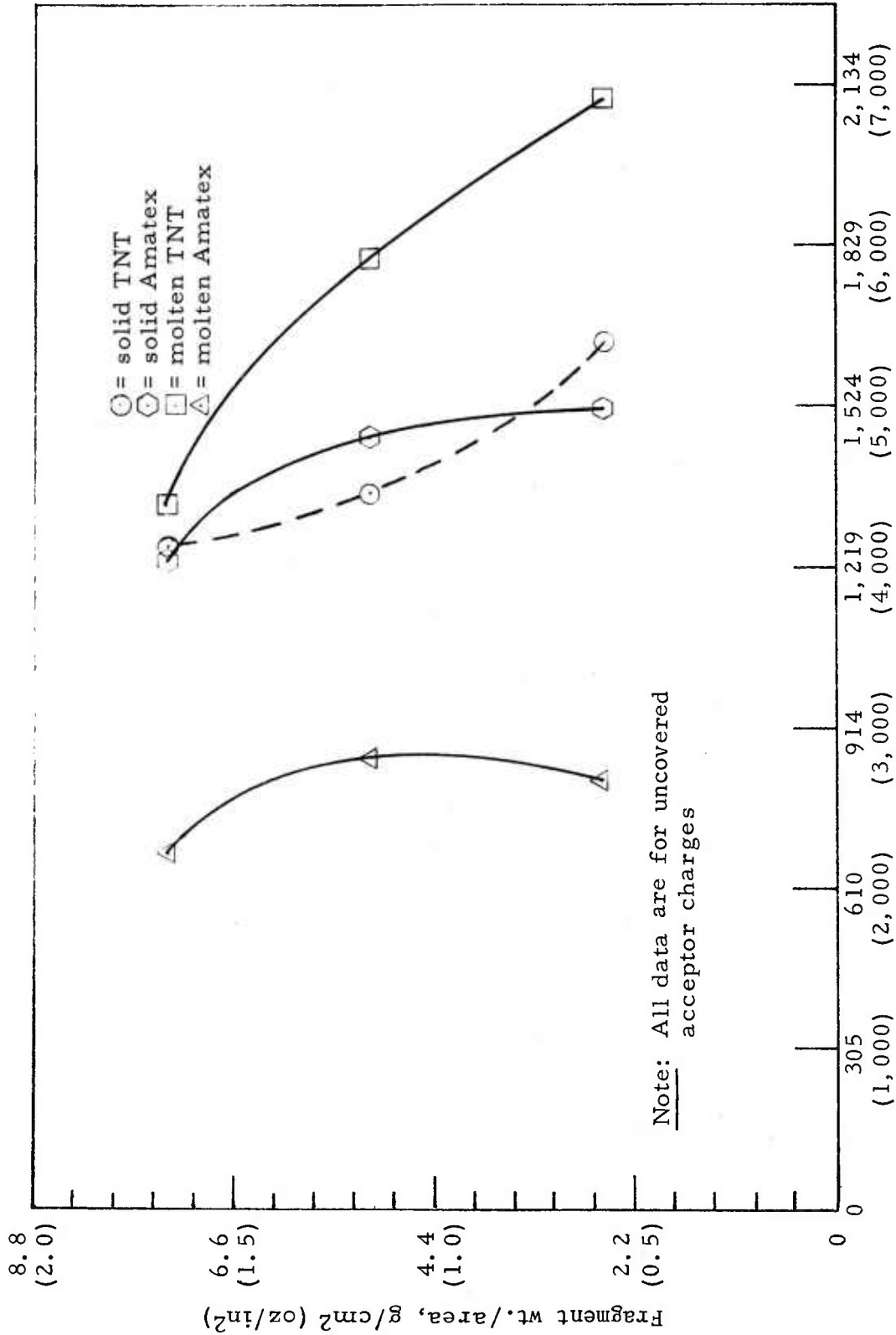


Figure 20. Comparison of minimum velocity for detonation of molten and solid TNT and Amatex as a function of fragment weight per unit area.

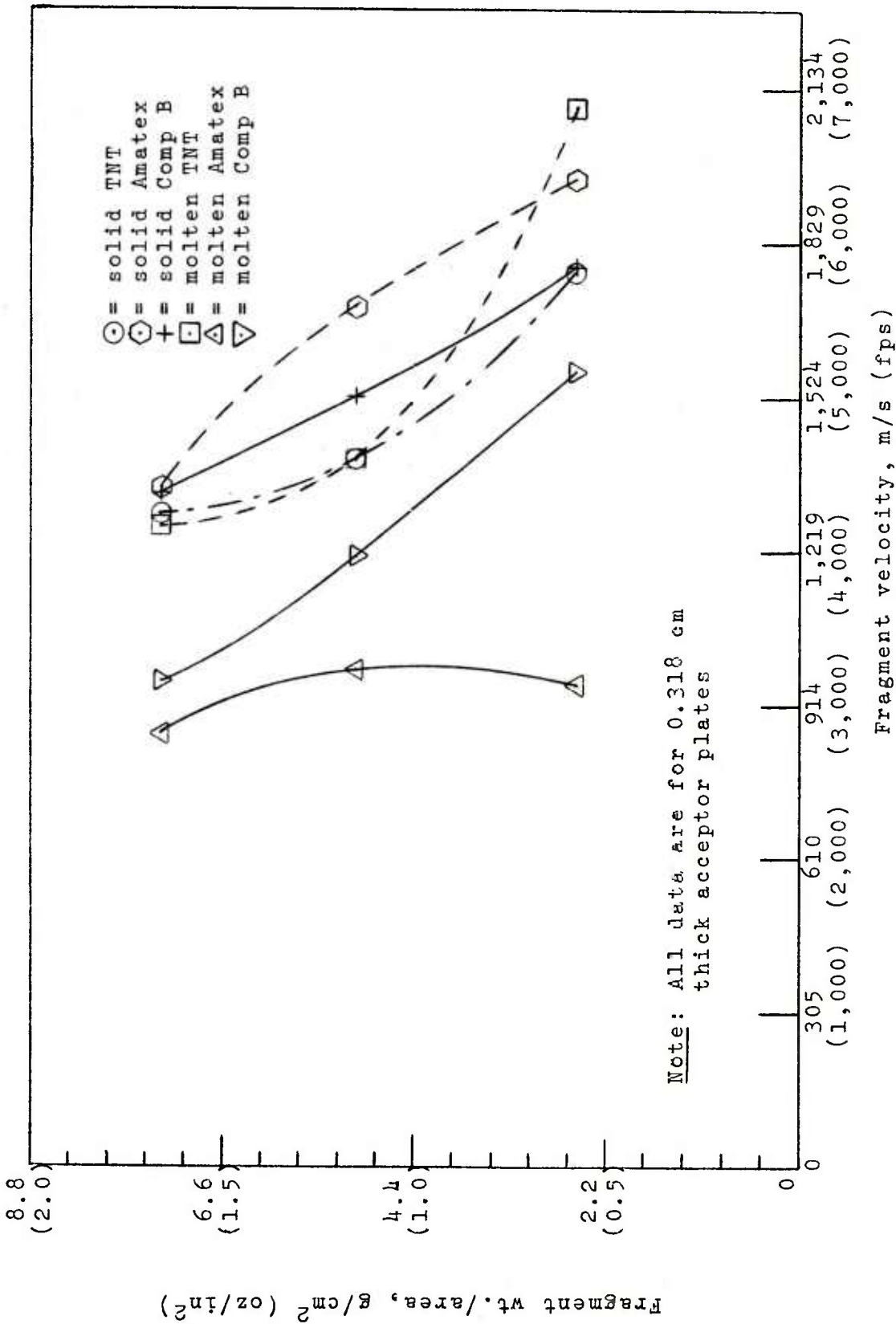


Figure 21. Comparison of test results for TNT, Composition B and Amatex

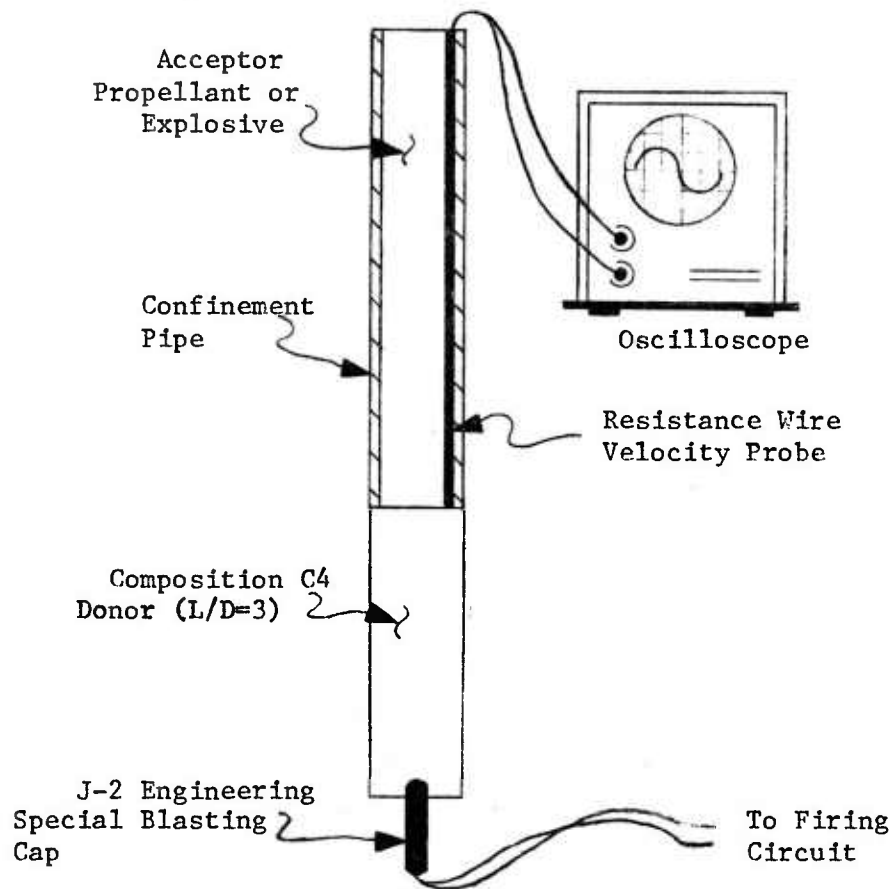


Figure 22. Critical diameter test setup.

DISTRIBUTION LIST

Commander  
U.S. Army Armament Research and  
Development Command  
ATTN: DRDAR-CG  
DRDAR-LCM-E  
DRDAR-LCM-S (20)  
DRDAR-SF  
DRDAR-TSS (5)  
Dover, NJ 07801

Chairman  
Dept of Defense Explosive Safety Board (2)  
Room 856C, Hoffman Building I  
2461 Eisenhower Avenue  
Alexandria, VA 22331

Administrator  
Defense Technical Information Center  
ATTN: Accessions Division (12)  
Cameron Station  
Alexandria, VA 22314

Commander  
Department of the Army  
Office, Chief of Research, Development  
and Acquisition  
ATTN: DAMA-CSM-P  
Washington, DC 20310

Office, Chief of Engineers  
ATTN: DAEN-MCZ  
Washington, DC 20314

Commander  
U.S. Army Materiel Development  
and Readiness Command  
ATTN: DRCSF  
DRCDE  
DRCRP  
DRCIS  
5001 Eisenhower Avenue  
Alexandria, VA 22333

Commander  
DARCOM Installations and Services Agency  
ATTN: DRCIS-RI  
Rock Island, IL 61299

Director  
Industrial Base Engineering Activity  
ATTN: DRXIB-MT and EN  
Rock Island, IL 61299

Commander  
U.S. Army Materiel Development  
and Readiness Command  
ATTN: DRCPM-PBM  
DRCPM-PBM-T  
DRCPM-PBM-L (2)  
DRCPM-PBM-E (2)  
DRCPM-PBM-LN-CE  
Dover, NJ 07801

Commander  
U.S. Army Armament Materiel  
Readiness Command  
ATTN: DRSAR-SF (3)  
DRSAR-SC  
DRSAR-EN  
DRSAR-IRC  
DRSAR-RD  
DRSAR-IS  
DRSAR-ASF  
DRSAR-LEP-L  
Rock Island, IL 61299

Director  
DARCOM Field Safety Activity  
ATTN: DRXOS-ES (2)  
Charlestown, IN 47111

Commander  
Volunteer Army Ammunition Plant  
Chattanooga, TN 37401

Commander  
Kansas Army Ammunition Plant  
Parsons, KS 67357

Commander  
Newport Army Ammunition Plant  
Newport, IN 47966

Commander  
Badger Army Ammunition Plant  
Baraboo, WI 53913

Commander  
Indiana Army Ammunition Plant  
Charlestown, IN 47111

Commander  
Holston Army Ammunition Plant  
Kingsport, TN 37660

Commander  
Lone Star Army Ammunition Plant  
Texarkana, TX 75501

Commander  
Milan Army Ammunition Plant  
Milan, TN 38358

Commander  
Iowa Army Ammunition Plant  
Middletown, IA 52638

Commander  
Joliet Army Ammunition Plant  
Joliet, IL 60436

Commander  
Longhorn Army Ammunition Plant  
Marshall, TX 75760

Commander  
Louisiana Army Ammunition Plant  
Schreveport, LA 71130

Commander  
Ravenna Army Ammunition Plant  
Ravenna, OH 44266

Commander  
Newport Army Ammunition Plant  
Newport, IN 47966

Commander  
Radford Army Ammunition Plant  
Radford, VA 24141

Division Engineer  
U.S. Army Engineer Division, Huntsville  
ATTN: HNDCD  
PO Box 1600, West Station  
Huntsville, AL 35809

Division Engineer  
U.S. Army Engineer Division, Southwestern  
ATTN: SWDCD  
1200 Main Street  
Dallas, TX 75202

Division Engineer  
U.S. Army Engineer Division, Missouri River  
ATTN: MRDCD  
PO Box 103, Downtown Station  
Omaha, NE 68101

Division Engineer  
U.S. Army Engineer Division, North Atlantic  
ATTN: NADCD  
90 Church Street  
New York, NY 10007

Division Engineer  
U.S. Army Engineer Division, South Atlantic  
30 Pryor Street, S.W.  
Atlanta, GA 30303

District Engineer  
U.S. Army Engineer District, Norfolk  
803 Front Street  
Norfolk, VA 23510

District Engineer  
U.S. Army Engineer District, Baltimore  
PO Box 1715  
Baltimore, MD 21203

District Engineer  
U.S. Army Engineer District, Omaha  
215 N. 17th Street  
Omaha, NE 68102

District Engineer  
U.S. Army Engineer District, Philadelphia  
Custom House  
2nd and Chestnut Street  
Philadelphia, PA 19106

District Engineer  
U.S. Army Engineer District, Fort Worth  
PO Box 17300  
Fort Worth, TX 76102

District Engineer  
U.S. Army Engineer District, Kansas  
601 E. 12th Street  
Kansas City, MO 64106

District Engineer  
U.S. Army Engineer District, Sacramento  
650 Capitol Mall  
Sacramento, CA 95814

District Engineer  
U.S. Army Engineer District, Mobile  
PO Box 2288  
Mobile, AL 36628

Commander  
U.S. Army Construction Engineering  
Research Laboratory  
Champaign, IL 61820

Commander  
Dugway Proving Ground  
ATTN: STEDP-MT-DA-HD (2)  
Dugway, UT 84022

Civil Engineering Laboratory  
Naval Construction Battalion Center  
ATTN: L51  
Port Hueneme, CA 93043

Commander  
Naval Facilities Engineering Command  
(Code 04, J. Tyrell)  
200 Stovall Street  
Alexandria, VA 22322

Commander  
Atlantic Division  
Naval Facilities Engineering Command  
Norfolk, VA 23511

Commander  
Chesapeake Division  
Naval Facilities Engineering Command  
Building S7  
Washington Navy Yard  
Washington, DC 20374

Commander  
Northern Division  
Naval Facilities Engineering Command  
Building 77-L  
U.S. Naval Base  
Philadelphia, PA 19112

Commander  
Southern Division  
Naval Facilities Engineering Command  
ATTN: J. Watts  
PO Box 10068  
Charleston, SC 29411

Commander  
Western Division  
Naval Facilities Engineering Command  
ATTN: W. Moore  
San Bruno, CA 94066

Commander  
Naval Ammunition Depct  
Naval Ammunition Production  
Engineering Center  
Crane, IN 47522

Technical Library  
ATTN: DRDAR-CLJ-L  
Aberdeen Proving Ground, MD 21010

Technical Library  
ATTN: DRDAR-TSB-S  
Aberdeen Proving Ground, MD 21005

Benet Weapons Laboratory  
Technical Library  
ATTN: DRDAR-LCB-TL  
Watervliet, NY 12189

Ammann and Whitney (10)  
2 World Trade Center  
New York, NY 10048

Weapon System Concept Team/CSL  
ATTN: DRDAR-ACW  
Aberdeen Proving Ground, MD 21010

U.S. Army Materiel Systems Analysis Activity  
ATTN: DRXSY-MP  
Aberdeen Proving Ground, MD 21005